41540R03

KINETICS OF SLURRY PHASE FISCHER-TROPSCH SYNTHESIS

Third Annual Technical Progress Report

Reporting Period Start Date: 10/01/2004

Reporting Period End Date: 09/30/2005

Report prepared by:

Dr. Dragomir B. Bukur (Professor, PI)

Dr. Gilbert F. Froment (Research Professor, Co-PI)

Tomasz Olewski (MSc., Research Technician)

Department of Chemical Engineering
Texas A&M University
College Station, TX 77843-3122

Date Report was issued: January 27, 2006

Grant No. DE-FG26-02NT41540

Texas A&M University
1260 TAMU
College Station, TX 77843-1260

Prepared for

The U.S. Department of Energy
University Coal Research Program
National Energy Technology Laboratory
Project Officer: Shelby Rogers

Disclaimer

Abstract

This report covers the third year of this research grant under the University Coal Research program. The overall objective of this project is to develop a comprehensive kinetic model for slurry phase Fischer-Tropsch synthesis (FTS) on iron catalysts. This model will be validated with experimental data obtained in a stirred tank slurry reactor (STSR) over a wide range of process conditions. The model will be able to predict molar flow rates and concentrations of all reactants and major product species (H_2O, CO_2, linear 1- and 2-olefins, and linear paraffins) as a function of reaction conditions in the STSR.

During the reporting period we utilized experimental data from the STSR, that were obtained during the first two years of the project, to perform vapor-liquid equilibrium (VLE) calculations and estimate kinetic parameters. We used a modified Peng-Robinson (PR) equation of state (EOS) with estimated values of binary interaction coefficients for the VLE calculations. Calculated vapor phase compositions were in excellent agreement with experimental values from the STSR under reaction conditions. Occasional discrepancies (for some of the experimental data) between calculated and experimental values of the liquid phase composition were ascribed to experimental errors. The VLE calculations show that the vapor and the liquid are in thermodynamic equilibrium under reaction conditions.

Also, we have successfully applied the Levenberg-Marquardt method (Marquardt, 1963) to estimate parameters of a kinetic model proposed earlier by Lox and Froment (1993b) for FTS on an iron catalyst. This kinetic model is well suited for initial studies where the main goal is to learn techniques for parameter estimation and statistical analysis of estimated values of model parameters. It predicts that the chain growth parameter (α) and olefin to paraffin ratio are independent of carbon number, whereas our experimental data show that they vary with the carbon number. Predicted molar flow rates of inorganic species, n-paraffins and total olefins were generally not in good agreement with the corresponding experimental values. In the future we'll use kinetic models based on non-constant value of α.

TABLE OF CONTENTS

	Page
Introduction	5
Current Status	6
Experimental	7
Results and Discussion	8
Vapor-Liquid Equilibrium	8
VLE Calculations for Binary Systems	9
VLE Calculations for FTS in the STSR	10
Kinetic Models and Parameter Estimation	12
Kinetic Model	12
Parameter Estimation Methodology	16
Results from Parameter Estimation	18
Activation Energies	20
Conclusions	21
Future Work	22
Acknowledgements	22
References	23
Tables	25
Figures	31
Notation	48
Appendix A Modified Peng-Robinson Equation of State	51
Appendix B Critical properties of Durasyn 164 oil	53
Appendix C Calculation of the vapor-liquid equilibrium	59

Introduction

The overall objective of this project is to develop a comprehensive kinetic model for slurry phase Fischer-Tropsch synthesis on iron catalysts. This model will be validated with experimental data obtained in a stirred tank slurry reactor (STSR) over a wide range of process conditions. This model will be able to predict concentrations of all reactants and major product species (H_2O, CO_2, linear 1- and 2-olefins, and linear paraffins) as a function of reaction conditions in the STSR. Kinetic model will be useful for preliminary reactor design and process economics study. The overall program is divided into several tasks, and their timetable and brief descriptions are:

Task 1. Development of Kinetic Models (November 1, 2002 - March 31, 2006)

Kinetic models will be formulated utilizing the current state-of-the-art understanding of reaction mechanisms for formation of reaction intermediates and hydrocarbon products. Models will be based on adsorption/desorption phenomena for reactants and product species. These models will be continually updated on the basis of experimental data obtained in Task 3, and subsequent data analysis in Task 4.

Task 2. Catalyst Synthesis (August 1, 2003 - October 30, 2003)

A precipitated iron catalyst with nominal composition 100 Fe/3 Cu/4 K/16 SiO_2 (in parts per weight) will be synthesized utilizing equipment and procedures developed in our laboratory at Texas A&M University (TAMU). As an alternative we may utilize a robust commercially available catalyst with similar performance characteristics to TAMU's catalyst.

Task 3. Experiments in a Stirred Tank Slurry Reactor (January 15, 2003 - March 31, 2004)

Experiments will be conducted in a 1 dm^3 stirred tank slurry reactor (STSR) over a wide range of process conditions of industrial significance. Synthesis gas feed H_2/CO molar ratio will vary from 0.67 (coal derived syngas) to 2 (natural gas derived syngas). Baseline conditions will be repeated periodically to assess the extent of catalyst deactivation.

Task 4. Model Discrimination and Parameter Estimation (March 1, 2005 – August 31, 2006)

Langmuir-Hinshelwood-Hougen-Watson (LHHW) approach and the concept of rate limiting step result in a large number of competing kinetic models. Discrimination between the rival models will be based upon the goodness of fit, supplemented with statistical tests on parameter values and the physicochemical meaningfulness of the estimated parameter values.

Current Status

Task 1. Development of Kinetic Models

The work on this task was initiated in June 2004. The initial work focused on adoption of one of the kinetic models of Lox and Froment (1993 a,b) to a stirred tank slurry reactor. The work on other models, with different rate-determining steps or mechanisms is in progress.

Task 2. Catalyst Synthesis

Instead of synthesizing a new batch of TAMU's precipitated catalyst 100 Fe/3 Cu/4 K/16 SiO_2 (in parts by weight) we used a precipitated iron catalyst prepared by Ruhrchemie AG (Oberhausen-Holten, Germany). This catalyst (LP 33/81) has a nominal composition 100 Fe/4.3 Cu/4.1 K/25 SiO_2 (in parts by weight) and it was used initially in fixed bed reactors at Sasol in South Africa. It has been tested extensively at TAMU (Bukur *et al*., 1990; Zimmerman and Bukur, 1990; Zimmerman *et al.*, 1992; Bukur *et al*., 1995), and was used in previous study of kinetics of Fischer-Tropsch (F-T) synthesis by Lox and Froment (Lox and Froment, 1993 a,b). It is a robust catalyst and its selectivity is similar to that of TAMU's catalyst.

Task 3. Experiments in a Stirred Tank Slurry Reactor

Three tests (runs SB-21903, SB-26203 and SB-28603) with the Ruhrchemie catalyst were conducted in a 1 dm^3 stirred tank slurry reactor (Autoclave Engineers) over a wide range of process conditions. Reaction temperature was 220, 240 or 260°C, pressure varied from 0.8 to 2.5 MPa, synthesis gas feed H_2/CO molar ratio was either 2/3 or 2, and the gas space velocity SV under the normal (standard) conditions (273.15°K, 101325 Pa) varied from 0.52 to 23.5 Ndm^3 g_{Fe}^{-1} h^{-1} to obtain wide range of conversions. Results and their qualitative analysis were described in detail in the Second Annual Report for this project (Bukur et al., 2005).

Task 4. Model Discrimination and Parameter Estimation

We have made progress in two areas related to this task. We have developed a method to calculate the vapor-liquid equilibrium (VLE) in the STSR, and we estimated kinetic parameters from our experimental data in the STSR using one of the kinetic models proposed by Lox and Froment (1993b).

The work on VLE modeling and calculations was initiated in November 2004 and was completed by the end of July 2005, whereas the work on parameter estimation was initiated in June 2005 and is still in progress. Our accomplishments in these two areas are described in the Results and Discussion Section of this report.

Experimental

Three tests (runs SB-21903, SB-26203 and SB-28603) were conducted in a 1 dm^3 stirred tank slurry reactor (Autoclave Engineers). A schematic of the experimental apparatus is shown in Figure 1. The feed gas flow rate was adjusted with a mass flow controller and passed through a series of oxygen removal, alumina and activated charcoal traps to remove trace impurities. After leaving the reactor, the exit gas passed through a series of high and low (ambient) pressure traps to condense liquid products. High molecular weight hydrocarbons (wax), withdrawn from a slurry reactor through a porous cylindrical sintered metal filter, and liquid products, collected in the high and low pressure traps, were analyzed by capillary gas chromatography (Varian 3400 gas chromatograph). Liquid products collected in the high and atmospheric pressure traps were first separated into an organic phase and an aqueous phase and then analyzed using different columns and temperature programmed methods (Varian 3400 gas chromatograph). The reactants and noncondensible products leaving the ice traps were analyzed on an on-line GC (Carle AGC 400) with multiple columns using both flame ionization and thermal conductivity detectors. A schematics of our product analysis procedure is shown in Figure 2. Further details on the experimental set up, operating procedures and product quantification can be found elsewhere (Bukur *et al*., 1990; Zimmerman and Bukur, 1990; Bukur *et al*., 1994; Bukur *et al*., 1996).

The Ruhrchemie catalyst (15 g in run SB-21903, 11.2 g in run SB-26203 and 25 g in run SB-28603) was calcined in air at 300°C and a fraction between 140-325 mesh was loaded into the reactor filled with 300-320 g of Durasyn 164 oil (a hydrogenated 1-decene homopolymer, ~ C_{30}). The catalyst was pretreated in CO at 280°C, 0.8 MPa (100 psig), and 3 NL/g-cat/h for 12 hours.

After the pretreatment the catalyst was tested initially at 260°C, 1.5 MPa (200 psig), 4 NL/g-Fe/h (where, NL/h, denotes volumetric gas flow rate at 0°C and 1 bar) using CO rich synthesis gas (H_2/CO molar feed ratio of 2/3). After reaching a stable steady state value (~60 h on stream) the catalyst was tested at different process conditions. A minimum length of time between changes in process conditions was 20 h.

Results and Discussion

Vapor-liquid equilibrium (VLE) calculations and kinetic parameter estimation were made utilizing experimental data from 27 sets of process conditions. These conditions are summarized in Table 1.

Vapor-Liquid Equilibrium

Introduction

Vapor and liquid phases are in equilibrium at the same temperature and pressure, when the fugacity of each constituent species is the same in all phases

$$\hat{f}_i^{\,v} = \hat{f}_i^{\,l} \tag{1}$$

Both, the vapor and liquid fugacities can be calculated using the corresponding fugacity coefficients, $\hat{\phi}_i$, from equation (2):

$$y_i \cdot \hat{\phi}_i^{\,v} \cdot P = x_i \cdot \hat{\phi}_i^{\,L} \cdot P \tag{2}$$

where x_i is a mole fraction of species *i* in the liquid and y_i is a mole fraction of species *i* in the gas. This expression of the vapor-liquid equilibrium is very convenient and relationship between gas and liquid composition can be expressed in terms of so called *K-value*

$$K_i = \frac{y_i}{x_i} = \frac{\hat{\phi}_i^{\,L}}{\hat{\phi}_i^{\,v}} \tag{3}$$

The fugacity coefficients $\hat{\phi}_i$ are calculated from an equation of state (EOS). Several equations of state have been used for this purpose. The following EOS have been used for VLE calculations in Fischer-Tropsch synthesis: Peng-Robinson (PR) equation of state (Marano and Holder, 1997;

Breman and Beenackers, 1996; Li and Froment, 1996), Redlich-Kwong (RK) EOS (Zimmerman, 1990) and Soave-Redlich-Kwong (SRK) EOS (Ahón *et al*., 2005). In this work we have chosen modified Peng-Robinson (PR) equation of state (EOS) for VLE calculations. According to the PR EOS the fugacity coefficient can be expressed as:

$$\ln\hat{\phi}_i = \frac{b_i}{b}(Z-1) - \ln(Z-B) + \frac{A}{2\sqrt{2}B}\left(\frac{b_i}{b} - \frac{2\sum_j z_j a_{ij}}{a}\right)\ln\left(\frac{Z+\left(1+\sqrt{2}\right)B}{Z+\left(1-\sqrt{2}\right)B}\right) \qquad (4)$$

where z is a mole fraction of species in the liquid phase, x, or in the gas phase, y. Definitions of other symbols (A, B, Z, a, a_{ij}, b and b_i) and additional explanations can be found in Appendix A.

In order to get good agreement between the PR EOS predictions and experimental data for inorganic species (H_2, CO, CO_2, H_2O) in higher molecular weight hydrocarbons two modifications of the PR EOS were made. The first modification deals with changes in the acentric factor function, $f_i(\varpi)$, from the original formulation (eqn. A.9 in Appendix A) to the extended form (eqn. A.10) proposed by Li and Froment (1996). The binary interaction factors k_{ij} (Appendix A, eqn. A.3) were estimated utilizing experimental data from literature on solubility of inorganic species in various hydrocarbons. Critical properties (the critical temperature and pressure) and acentric factor ω of inorganic species and linear paraffins and olefins (up to C_{20}) were taken from Poling *et al*. (2001) and Nikitin *et al*. (1997). For higher molecular weight hydrocarbons (> C_{20}) we used equations from Gao *et al.* (2001). The critical temperature and pressure of the start-up fluid (Durasyn) were estimated from Joback's group contribution methods (Joback, 1984; Joback and Reid, 1987), whereas the acentric factor was estimated from Lee and Kessler (1975). Details of calculation procedure for estimation of properties of Durasyn are given in Appendix B.

VLE Calculations for Binary Systems

The binary interaction factors k_{ij} for inorganic species (H_2, CO, CO_2, H_2O) in hydrocarbons were estimated from experimental VLE data in binary systems from the literature (Peter and Weinert, 1955; Calderbank *et al*., 1963; Gasem and Robinson, 1985; Nettelhoff *et al*. 1985; Chao and Lin,

1988; Miller and Ekstrom, 1990; Breman *et al*., 1994; Park *et al*., 1995; Gao *et al*., 1999). Experimental conditions employed in these studies are summarized in Table 2.

The interaction factors were optimized to obtain the best agreement with reported experimental K_i values ($K_i = y_i/x_i$). Comparisons of calculated (from the PR EOS with optimized k_{ij} values) and experimental K values for different binary systems and different conditions (P and T) are shown in Figures 3-9. It can be seen that there is excellent agreement between calculated K values and the experimental ones for permanent gases (H_2, CO, CO_2) in different solvents over a wide range of pressures and temperatures (Figures 3-8). Discrepancies between calculated and experimental values for water (Fig. 9) are caused by large differences in reported experimental K values by different authors. In several figures (3-5, 7 and 9) we have also included predictions based on Nettelhoff et al. (1985) correlation for Henry's law constant. This correlation was obtained from authors' experimental data with H_2 and CO in Vestowax (hydrocarbon wax) and Peter and Weinert's (1955) data in hydrocarbon wax (molecular weight = 345). Nettelhoff et al. (1985) correlation for Henry's law constant does not account for the effects of pressure and molecular weight of solvent, and the predicted K values are usually lower than the experimental ones. The use of PR EOS with adjustable interaction factors provides a much better fit of the experimental data over a wide range of conditions.

The optimized values of interaction factors vary with molecular weight of solvent, but are weak functions of temperature (200-300 C) and pressure (10-30 bar). Average values of the interaction coefficients k_{ij} in different hydrocarbons are summarized in Table 3, and their variation with carbon number is shown graphically in Figure 10. In subsequent VLE calculations the data from Figure 10 were used to obtain interaction factors of the inorganic species in hydrocarbons with carbon numbers between 20 and 36 by linear interpolation.

VLE Calculations for FTS in the STSR

We used the PR EOS with the above-mentioned modifications (acentric factor function and the binary interaction coefficients for inorganic components with hydrocarbons having more than 20 carbon atoms) to perform VLE calculations for our experiments in the STSR (Table 1). The following species were taken into account in the VLE calculations: inorganic species (H_2, CO, CO_2, H_2O), n-paraffins (C_1-C_{20}), 1-olefins (C_2-C_{15}), Durasyn (C_{30}) and two pseudo-components: C_{21}^+ paraffins and unanalyzed wax (with critical properties and acentric factor of C_{30} n-paraffin).

Thus, the VLE calculations were done for a two-phase mixture of 41 components (species). Interaction factors (k_{ij}) were used for each combination of inorganic species with one of the following high molecular weight hydrocarbons: C_{20} paraffin, C_{21}^{+} paraffins (represented by a component having the average molecular weight of the mixture), unanalyzed wax (C_{30} n-paraffin) and Durasyn. Thus, for each inorganic species there are four non-zero interaction factors. The interaction factors for all other species were set to zero. Detailed explanations, equations and the computational algorithm for the VLE calculations are given in the Appendix C.

The VLE calculations were made for all 27 sets of process conditions (mass balances) shown in Table 1. Representative results (four mass balances) are shown in Figures 11 and 12. In each of these figures calculated mole fractions of hydrocarbon species (C_1-C_{20} n-paraffins, and C_2-C_{15} 1-olefins) in the liquid (x_i) and vapor (y_i) phase are shown together with the corresponding experimental values. In all cases (including the ones not shown in these two figures) there is a very good agreement between the calculated and experimental values for the vapor phase composition, whereas the agreement between the calculated and experimental values of mole fractions in the liquid phase ranges from fairly good (Figure 11) to poor (Figure 12). The reason for larger discrepancies (calculated vs. experimental) for the liquid phase components is that the amounts of Durasyn and wax (as well as their ratio) withdrawn from the reactor are not measured accurately.

It should be noted that lower molecular weight hydrocarbons (C_1-C_9) and inorganic species are not detected experimentally in the liquid phase, and thus their experimental values are not shown in Figures 11 and 12. To account for the absence of lighter components in the liquid phase one can use the normalized calculated mole fractions (xnorm in Figures 11 and 12) for comparison with the experimental mole fractions (for the liquid phase only). The normalized values of the calculated liquid phase mole fractions were calculated from the following equation:

$$x_i^{norm} = \frac{x_i^{calc}}{\sum_{i \in \Delta} x_i^{calc}} \tag{5}$$

where Δ means components, which were measured experimentally in the liquid phase. As can be seen in Figures 11 and 12, the normalization does not have significant effect on results because the measured components account for more than 90% of the total liquid phase.

We conclude that the VLE calculations show that the vapor and liquid phase are in thermodynamic equilibrium during Fischer-Tropsch synthesis in the STSR. Discrepancies between calculated and experimental liquid phase compositions are attributed to experimental errors.

Kinetic Models and Parameter Estimation

Kinetic Model

The model reported as the best by Lox and Froment (marked by symbol ALII in Lox and Froment, 1993b) for their operating conditions (high H_2/CO feed ratio of 3) has been selected for initial estimation of kinetic parameters from our experimental data in the stirred tank slurry reactor (STSR). It accounts for formation of carbon dioxide, water, paraffins and total olefins (it does not distinguish between 1- and 2-olefins) as well as consumption of hydrogen and water. This model predicts a constant value for the chain growth probability factor, α, whereas we know that our experimental data (Bukur et al., 2005) show that α is not constant (i.e. it varies with carbon number). However, a simplified form of this model contains only five parameters at isothermal conditions. Because of its relative simplicity this model is well suited for initial studies where the main goal is to learn techniques for parameter estimation and statistical analysis of estimated values of model parameters. The same techniques and computer codes will be utilized in the future work, where different types of kinetic models will be investigated.

The ALII model utilizes Langmuir-Hinshelwood-Hougen-Watson (LHHW) approach and the concept of rate-determining steps (RDS). The elementary steps (reactions) for Fischer-Tropsch synthesis (FTS) and Water-Gas-Shift (WGS) reaction are shown in Tables 4 and 5, respectively. Reactant molecules are adsorbed on two types of active sites, one for FTS and the second for WGS reaction, where the surface reactions take place. The model assumes two RDS in each path of formation of paraffins and olefins in the Fischer-Tropsch reaction:

- adsorption of carbon monoxide (HC1) and desorption of the paraffin (HC5) in the reaction path leading to the paraffins,

- adsorption of carbon monoxide (HC1) and desorption of the olefin (HC6) in the reaction path leading to the olefins,

and one RDS for the WGS reaction path:

- reaction of an adsorbed carbon monoxide with adsorbed hydroxyl group (WGS2 in Table 5).

The resulting equations for rates of formation of n-paraffins, olefins and carbon dioxide in terms of partial pressures of reactants (H_2 and CO) and products (CO_2 and H_2O) are:

Rates of paraffin formation

$$R_{C_nH_{2n+2}} = \frac{k_{HC5} \cdot C_{l_1,tot} \cdot K_{HC7}^{0.5} \cdot p_{H_2}^{1.5} \cdot \frac{k_{HC1} \cdot p_{CO}}{k_{HC1} \cdot p_{CO} + k_{HC5} \cdot p_{H_2}} \cdot (\alpha)^{n-1}}{DENOMHCIII} \qquad (6)$$

$$n \geq 1$$

Rates of olefin formation

$$R_{C_nH_{2n}} = \frac{k_{HC6} \cdot C_{l_1,tot} \cdot K_{HC7}^{0.5} \cdot p_{H_2}^{0.5} \cdot \frac{k_{HC1} \cdot p_{CO}}{k_{HC1} \cdot p_{CO} + k_{HC5} \cdot p_{H_2}} \cdot (\alpha)^{n-1}}{DENOMHCIII} \qquad (7)$$

$$n \geq 2$$

where *DENOMHCIII* is

$$DENOMHCIII = 1 + K_{HC7}^{0.5} \cdot p_{H_2}^{0.5} +$$
$$+ \left(\frac{k_{HC1} \cdot p_{CO}}{k_{HC1} \cdot p_{CO} + k_{HC5} \cdot p_{H_2}} \cdot \frac{k_{HC1} \cdot p_{CO} + k_{HC5} \cdot p_{H_2} + k_{HC6}}{k_{HC5} \cdot p_{H_2} + k_{HC6}} \right) \times \qquad (8)$$
$$\times \left(\frac{K_{HC7}^{0.5}}{K_{HC2} \cdot K_{HC3} \cdot K_{HC4}} \cdot \frac{p_{H_2O}}{p_{H_2}^{1.5}} + \frac{K_{HC7}^{0.5}}{K_{HC3} \cdot K_{HC4}} \cdot \frac{1}{p_{H_2}^{0.5}} + \frac{K_{HC7}^{0.5}}{K_{HC4}} \cdot p_{H_2}^{0.5} + K_{HC7}^{0.5} \cdot p_{H_2}^{0.5} \right)$$

and α (chain grow probability factor) is

$$\alpha = \frac{k_{HC1} \cdot p_{CO}}{k_{HC1} \cdot p_{CO} + k_{HC5} \cdot p_{H_2} + k_{HC6}} \qquad (9)$$

Rate of carbon dioxide formation:

$$R_{CO_2} = \frac{k_v \cdot \left(\frac{p_{H_2O} \cdot p_{CO}}{p_{H_2}{}^{0.5}} + - \frac{1}{K_{WGS}} \cdot p_{CO_2} \cdot p_{H_2}{}^{0.5} \right) \cdot C_{l_2,tot}{}^2}{(DENOMWGSII)^2} \tag{10}$$

where pseudo-reaction constant k_v is given by

$$k_v = k_{2,WGS} \cdot \frac{K_{1,WGS} \cdot K_{4,WGS}}{K_{5,WGS}{}^{0.5}} \tag{11}$$

and

$$\begin{aligned} DENOMWGSII = 1 + K_{1,WGS} \cdot p_{CO} + \frac{K_{4,WGS}}{K_{5,WGS}{}^{0.5}} \cdot \frac{p_{H_2O}}{p_{H_2}{}^{0.5}} + \\ + \frac{K_{5,WGS}{}^{0.5}}{K_{3,WGS}} \cdot p_{CO_2} \cdot p_{H_2}{}^{0.5} + K_{5,WGS}{}^{0.5} \cdot p_{H_2}{}^{0.5} \end{aligned} \tag{12}$$

Lox and Froment assumed that the total concentration of active sites could be approximated by a sum of surface concentrations of intermediates involved in the irreversible reactions, i.e.

$$C_{l_1,tot} = C_{Hl_1} + \sum_{n=1}^{\infty} C_{C_nH_{2n+1}l_1} \tag{13}$$

$$C_{l_2,tot} = C_{l2} + C_{OHl_2} \tag{14}$$

where $C_{l_1,tot}$ and $C_{l_2,tot}$ are total concentrations of the active sites of type l_1 or l_2 on the surface of the catalyst; C_{Hl_1}, $C_{C_nH_{2n+1}l_1}$, C_{OHl_2} are concentrations of adsorbed species on the surface and C_{l2} is a concentration of vacant active sites for the WGS reaction. The FTS reactions take place on active sites of type l_1 whereas the WGS reaction on sites of type l_2.

Next, the terms $k_{HCx} \cdot C_{l_1,tot}$ are lumped into new kinetic coefficients, and notation for the rate constant for CO adsorption (Reaction HC1 in Table 4) is changed:

$k_{HC1} \cdot C_{l_1,tot} \equiv k_{CO,HC}$, $k_{\mathrm{HC5}} \cdot C_{l_1,tot} \equiv k_{\mathrm{t,p}}$ and $k_{\mathrm{HC6}} \cdot C_{l_1,tot} \equiv k_{\mathrm{t,o}}$.

With the above simplifications and changes in notation reaction rates of formation of paraffins, olefins, carbon dioxide and water, and rates of consumption of hydrogen and CO are given by equations (15-21):

Paraffin formation rates:

$$R_{C_nH_{2n+2}} = \frac{k_{t,p} \cdot p_{H_2} \cdot \frac{k_{CO,HC} \cdot p_{CO}}{k_{CO,HC} \cdot p_{CO} + k_{t,p} \cdot p_{H_2}} \cdot (\alpha)^{n-1}}{1 + \frac{k_{CO,HC} \cdot p_{CO}}{k_{CO,HC} \cdot p_{CO} + k_{t,p} \cdot p_{H_2}} \cdot \frac{1}{1-\alpha}}, \quad n \geq 1 \tag{15}$$

Olefin formation rates:

$$R_{C_nH_{2n}} = \frac{k_{t,o} \cdot \frac{k_{CO,HC} \cdot p_{CO}}{k_{CO,HC} \cdot p_{CO} + k_{t,p} \cdot p_{H_2}} \cdot (\alpha)^{n-1}}{1 + \frac{k_{CO,HC} \cdot p_{CO}}{k_{CO,HC} \cdot p_{CO} + k_{t,p} \cdot p_{H_2}} \cdot \frac{1}{1-\alpha}}, \quad n \geq 2 \tag{16}$$

where p_i is partial pressure of component i and the chain growth parameter α is:

$$\alpha = \frac{k_{CO,HC} \cdot p_{CO}}{k_{CO,HC} \cdot p_{CO} + k_{t,p} \cdot p_{H_2} + k_{t,o}} \tag{17}$$

The units of kinetic rate coefficients are:

$$\langle k_{CO,HC} \rangle = \frac{mol}{s \cdot g_{cat} \cdot bar} \qquad \langle k_{t,p} \rangle = \frac{mol}{s \cdot g_{cat} \cdot bar} \qquad \langle k_{t,o} \rangle = \frac{mol}{s \cdot g_{cat}}$$

These parameters correspond to k_1, k_5 and k_6 in Table IX in Lox and Froment (1993b).

Rate of carbon dioxide formation is:

$$R_{CO_2} = \frac{k_v^{'} \cdot \left(p_{H_2O} \cdot p_{CO} \,/\, {p_{H_2}}^{0.5} - \frac{1}{K_{WGS}} \cdot p_{CO_2} \cdot {p_{H_2}}^{0.5} \right)}{\left(1 + K_v \cdot p_{H_2O} \,/\, {p_{H_2}}^{0.5} \right)^2} \tag{18}$$

where

$$k_v^{'} = k_{2,WGS} \cdot \frac{K_{CO,WGS} \cdot K_{H_2O,WGS}}{K_{H_2,WGS}^{0.5}} \cdot C_{l_2,tot}^{\ 2} \qquad \left\langle k_v^{'} \right\rangle = \frac{mol}{s \cdot g_{cat}} \cdot (bar)^{-1.5}$$

$$K_v = \frac{K_{H_2O,WGS}}{K_{H_2,WGS}^{0.5}} \qquad \langle K_v \rangle = (bar)^{-0.5}$$

These parameters correspond to k_v and K_v in Table IX in Lox and Froment (1993b).

If one assumes that the only products are n-paraffins, linear olefins, carbon dioxide and water, then the rates of formation of CO, H_2, and water can be expressed from the reaction stoichiometry as:

Rate of formation of carbon monoxide

$$R_{CO} = -[\sum_{n=1}^{50}(n \cdot R_{C_nH_{2n+2}}) + \sum_{n=1}^{50}(n \cdot R_{C_nH_{2n}}) + R_{CO_2}] \tag{19}$$

Rate of formation of hydrogen

$$R_{H_2} = -\sum_{n=1}^{50}((2n+1) \cdot R_{C_nH_{2n+2}}) - \sum_{n=1}^{50}(2n \cdot R_{C_nH_{2n}}) + \cdot R_{CO_2} \tag{20}$$

Rate of formation of water

$$R_{H_2O} = \sum_{n=1}^{50}(n \cdot R_{C_nH_{2n+2}}) + \sum_{n=1}^{50}(n \cdot R_{C_nH_{2n}}) - R_{CO_2} \tag{21}$$

Note that rates of formation of H_2 and CO will be negative. Also, this model predicts that rates of formation of n-paraffins and olefins, as well as the chain growth probability factor, are independent of carbon number (equations 15-17). This model predicts that the olefin to paraffin ratio is independent of carbon number, and that the carbon number distribution follows the ideal Schulz-Flory distribution.

Parameter Estimation Methodology

A simplified ALII model of Lox and Froment (1993b) has five kinetic parameters, three for the Fischer-Tropsch synthesis (FTS) reaction:

- adsorption of carbon monoxide, $k_{\mathrm{CO,HC}}$,

- desorption of a paraffin, $k_{t,p}$,

- desorption of an olefin, $k_{t,o}$,

and two parameters for the WGS reaction:

- constant containing the WGS rate constant $k_{\nu}^{'}$, and ratio of adsorption constants K_{ν}.

In equations (15) to (21) the unknowns are 5 kinetic constants, whereas partial pressures of hydrogen, carbon monoxide, carbon dioxide and water are known from the VLE calculations ($p_i = y_i \cdot P$).

Parameters are estimated by minimizing an objective function, S. We used the objective function that minimizes the sum of squares of residuals of reaction rates:

$$S = \sum_{h=1}^{v} \sigma_{h,h} \cdot \sum_{i=1}^{n} \left(\hat{R}_{i,h} - R_{i,h} \right)^2 \tag{22}$$

where $\hat{R}$ means experimental, whereas R represents calculated reaction rate. $\sigma_{h,h}$ are diagonal elements of the inverse of the error covariance matrix. When replicate experiments are available the weighting factors can be calculated (Froment and Bischoff, 1990) as:

$$\sigma_{h,h} = \left(\frac{\sum_{i=1}^{n_e} \left(\hat{R}_{i,h} - \overline{R}_h \right)^2}{n_e - 1} \right)^{-1} \tag{23}$$

where $\overline{R}_h$ represents the average value of response *h* over n_e replicate experiments (n_e is equal to 3 in our case), *n* is a number of experiments at constant temperature and *v* is a number of components (in our case: CO, CO_2, H_2, H_2O, twenty n-paraffins $C_{1\text{-}20}$, fourteen 1-olefins $C_{2\text{-}14}$ and pseudo-component $C_{21\text{-}50}$). Reaction rate of pseudo-component C_{21}^{+} is calculated as follows:

$$R_{21+} = \sum_{i=21}^{50} R_i \tag{24}$$

When there is insufficient information about the nature of errors in experimental measurements, another weighting factor can be used. In such cases, the simplest form of the weighting factor is the inverse of squared mean response of the j^{th} variable (Englezos and Kalogerakis, 2001):

$$\sigma_{j,j} = \left(\frac{1}{n} \cdot \sum_{i=1}^{n} \hat{R}_{ij} \right)^{-2} \tag{25}$$

When the weighting factors are not used in equation (22) then the σ matrix is the identity matrix, i.e. $\sigma_{h,h} = 1$.

Minimization of the objective function was done by the Levenberg-Marquardt method (Marquardt, 1963) which is an improved form of the Newton-Gauss optimization technique. The minimization procedure consists of the following steps:

1. Initial guess of unknown parameters k^0 is made. The corresponding reaction rates are calculated using the assumed values of kinetic parameters and the objective function is evaluated.
2. New (improved) values of kinetic parameters k^i are found by the Marquardt method.
3. New values of reaction rates and the objective function are obtained.
4. If the current (new) value of the objective function is smaller or equal to the previous (old) one then go to step 5. If not, go to step 2 and keep iterating until a criterion for minimization is achieved, i.e.:

$$S\left(k^{i+1}\right) \leq S\left(k^{i}\right)$$

5. Stop iterations when the difference between the current and the previous value of the objective function is smaller then the desired convergence criterion, ε_p.

$$\left| S\left(k^{i+i}\right) - S\left(k^{i}\right) \right| \leq \varepsilon_p$$

If the convergence is not achieved, go back to step 2 and iterate until the convergence criterion is achieved. Numerical value of ε_p was set to 10^{-6}.

Results from Parameter Estimation

Estimated values of kinetic parameters obtained using the objective function (22) with weighting factors equal to one and with weighting factors calculated using equation (25) are shown in Table 6. As can be seen from this table the rate constant for olefin formation, $k_{t,0}$, estimated assuming that all weighting factors are equal to one, is negative for data at 220°C and 260°C. Therefore, this approach ($\sigma_{h,h} = 1$ in equation (22)) yields unsatisfactory results. The use of

weighting factors calculated from equation (25) results in positive values for all five rate constants at all three temperatures (Table 6). In the remainder of this report we describe only the results that were obtained using the weighting factors calculated as the inverse of squared mean response of the j^{th} variable (Eq. (25)).

Statistical parameters associated with calculated rate constants are shown in Table 7. Approximate 95% confidence intervals for the WGS kinetic parameters k'_v and K_v show that these parameters are not significantly different from zero (lower 95% confidence interval gives negative values), whereas mean values of three kinetic parameters for the FTS are statistically reliable.

Representative parity plots, for reaction temperature of 260°C, are shown in Figures 13 and 14. They show comparison of calculated and experimental reaction rates. Calculated and experimental rates for inorganic species (H_2, CO, CO_2 and H_2O) are shown in Figure 13, whereas results for hydrocarbons are shown in Figure 14. In the case of H_2 and CO, the absolute rates are shown in Fig. 13. If the model fits the data, experimental points would lie on a straight line with 45° slope. However, almost all of the calculated reaction rates are smaller then the experimental ones (Figures 13 and 14). Results for various hydrocarbon species (Fig. 14) are shown with two different scales. As can be seen in this figure the Lox and Froment's (1993b) ALII model does not predict accurately the formation rates of various hydrocarbons (individual species as well as lumped species). Detailed comparison of predicted and experimental formation rates of individual species (C_1-C_{20} n-paraffins, and C_2-C_{15} olefins) is shown in Figure 15. Experimental values are represented by points, whereas solid lines are model predictions. Model predictions are represented by straight lines on a semi-logarithmic plot (log Rate vs. Carbon number) whereas experimental points have curvatures. It can be seen that the model does not predict accurately the observed reaction rates of individual hydrocarbons.

Figure 16 shows carbon number distribution of hydrocarbon products on a semi-logarithmic scale (logarithm of reaction rate of hydrocarbons containing n carbon atoms vs. carbon number). The model yields a straight line, whereas experimental data show nonlinear dependence on carbon number. The model predictions reflect the ideal Anderson-Schulz-Flory (ASF) distribution characterized by a constant value of the chain growth probability factor α, whereas experimental data show that α varies with carbon number.

Predicted and experimental values of olefin to n-paraffin reaction rates (Olefin to paraffin ratio) as a function of carbon number are shown in Figure 17. The model predictions are represented by a horizontal line, whereas experimental values are carbon number dependent. Clearly the model fails to predict the observed experimental trends both qualitatively and quantitatively.

Activation Energies

From estimated values of kinetic parameters at three reaction temperatures (Table 6, weighting factors from equation (25)) we have calculated the corresponding activation energies and frequency factors. The adsorption constant for carbon monoxide adsorption $k_{\mathrm{CO,HC}}$, desorption rate constant of n-paraffins $k_{\mathrm{t,p}}$, desorption rate constant of olefin $k_{\mathrm{t,o}}$ and the WGS reaction rate constant $k_{\nu}^{'}$ satisfy the Arrhenius equation:

$$k = A_0 \cdot e^{\frac{-E_a}{RT}} \tag{27}$$

where A_0 is a frequency factor, E_a is an activation energy, R is universal gas constant equal to *8.3144 kJ/mol* and T is temperature measured in *Kelvins*.

Numerical values of activation energies (E_a) are shown in Table 8. Statistical parameters shown in Table 8 are calculated for one degree of freedom ($n - p$, where n is number of independent values, data at temperatures: 220, 240 and 260°C, whereas p is a number of parameters, A_0 and E_a) and for statistical significance α equal to 0.05. Approximate 95% confidence intervals are large, due to the fact that there is only one degree of freedom in the estimation. However, the approximate confidence intervals indicate that estimated values of activation energies for carbon monoxide adsorption $E_{\mathrm{CO,HC}}$, n-paraffin formation $E_{\mathrm{t,p}}$, and olefin formation $E_{\mathrm{t,o}}$ are reliable, because they are all non-negative. The approximate confidence intervals for the WGS activation energy E_{ν} range from -585 to 1003. This means that the estimated value for E_{ν} (209 kJ/mol) is not significantly different from zero, and it has a small impact on the model result. Relatively small standard error value and high t-value imply that estimated parameter value is obtained with good accuracy. As can be seen, these conditions are satisfied for activation energies: $E_{\mathrm{CO,HC}}$, $E_{\mathrm{t,p}}$ and $E_{\mathrm{t,o}}$.

Activation energies for formation of paraffins ($E_{t,p}$) and olefins ($E_{t,o}$) can be compared with the corresponding values reported in the literature (Table 9). Reported values of the activation energy for the paraffin formation are between *70* and *112 kJ/mol*, and those for the olefin formation are *97 – 132 kJ/mol*. Activation energies from our data with the ALII kinetic model of Lox and Froment (1993b) are *121 kJ/mol* for paraffin formation, and *54 kJ/mol* for the olefin formation. The former is slightly higher than the upper bound from the literature, whereas the olefin formation activation energy value is about 50% lower than a typical value from the literature. The estimated activation energy for the WGS reaction (*209 kJ/mol*) is too high compared to the corresponding values in the literature (*28-137 KJ/mol*), and is not reliable as discussed earlier (lower 95% confidence interval gives negative value).

Conclusions

During the third year of the project we performed an analysis of experimental data collected earlier. Vapor-liquid equilibrium (VLE) calculations were made for 27 mass balances, and kinetic parameters were estimated from the same set of experimental data.

We have successfully implemented a method for calculation of VLE based on modified Peng-Robinson equation of state (PR EOS). First we estimated binary interaction factors k_{ij} for inorganic species (H_2, CO, CO_2 and H_2O) in high molecular weight hydrocarbons from an extensive set of experimental data from the literature, which cover the range of experimental conditions for FTS used in our study (220 – 260°C, 8 – 25bar). We were able to obtain an excellent fit of available experimental data for binary systems: H_2, CO or CO_2 in a hydrocarbon, whereas the experimental data for water in hydrocarbons are more sparse and scattered. Utilizing the modified PR EOS we performed VLE calculations for FTS reaction in the STSR, and compared calculated vapor phase and liquid phase compositions with the corresponding experimental values. Excellent agreement was obtained for the vapor phase composition, whereas we observed differences between the calculated and experimental liquid phase compositions for some mass balances. Experimental values of the liquid phase composition are difficult to measure accurately, due to difficulties in accurate quantification of the total amount of liquid withdrawn from the reactor and relative amounts of hydrocarbon wax and the start-up fluid (Durasyn). Overall, our calculations indicate that the vapor and liquid phase are in thermodynamic equilibrium during FTS in the STSR.

We utilized one of the kinetic models of Lox and Froment (model ALII in Lox and Froment, 1993b) for FTS and WGS reactions and estimated model parameters from experimental data in the STSR. The Levenberg-Marquardt method was employed for minimization of the objective function and kinetic parameter estimation. With a judicious choice of weighting factors in the objective function we were able to obtain non-negative values for all five model parameters. Statistical analysis of estimated values of model parameters revealed that kinetic parameters for FTS (3 parameters), as well as their corresponding activation energies, are statistically significant, whereas two parameters for the WGS reaction were not statistically significant. Predicted reaction rates of inorganic and hydrocarbon species were not in a good agreement with experimental data. This model predicts that the chain growth parameter (α) and olefin to paraffin ratio are independent of carbon number, whereas our experimental data show that they vary with the carbon number. Lox and Froment (1993b) developed kinetic models (based on different rate determining steps and/or reaction mechanisms) that predict variation of α with carbon number, and these models would be more suitable for our experimental data.

Future Work

Our plan for the next period is to continue working on development of kinetic models and estimation of model parameters from our experimental data in the STSR. The emphasis will be on kinetic models that account for 1-olefin readsorption reaction, and models that predict deviations from classical Schultz-Flory distribution, i.e. models that predict variations in chain growth probability and olefin to paraffin ratio with carbon number.

Acknowledgements

This work was supported by US DOE (University Coal Research Program) grant No. DE-FG26-02NT41540.

References

Ambrose, D. and C. Tsonopoulos, *J. Chem. Eng. Data*, 40, 531-546 (1995)

Ambrose, D., *"Correlation and Estimation of Vapor-Liquid Critical Properties. I. Critical Temperatures of Organic Compounds"*, National Physical Laboratory, Teddington, *NPL Rep. Chem*., 98 (1979)

Ambrose, D. and J. Walton, *Pure & Appl. Chem*., 61, 1395 (1989)

Ahon, V.R., E F. Costa Jr., J.E.P. Monteagudo, C.E. Fontes, E.C. Biscaia Jr., P.L.C. Lage, *Chemical Engineering Science*, 60, 677 (2005)

Bukur, D.B., S.A. Patel and X. Lang, *Appl. Catal.*, 61, 329 (1990)

Bukur, D. B., L. Nowicki and X.Lang, , *Chem. Eng. Sci*., 49, 4615 (1994)

Bukur, D. B., L. Nowicki, R. K. Manne and X. Lang, *J. Catal*., 155, 366 (1995)

Bukur, D. B., L. Nowicki and S. A. Patel, *Can. J. Chem. Eng*., 74, 399 (1996)

Bukur D.B., G.F. Froment, L. Nowicki, M. Nyapathi and X. Wang, *"Kinetics of Slurry Phase Fischer-Tropsch Synthesis"*, Second Annual Technical Progress Report for DOE, Contract No. DE-FG26-02NT41540, Texas A&M University, College Station, TX, January 2005

Breman, B. B., A. A. C. M. Beenackers, E. W. J. Rietjens and R. J. H., J. Stege, *Chem. Eng. Data*, 39, 647 (1994)

Breman, B. B. and A. A. Beenackers, *Ind. Eng. Chem. Res*., 35 (10), 3763 (1996)

Calderbank, P.H., F. Evans, R. Farley, G. Jepson and A. Poll, *Catalysis in Practice, IChemE,* 66 (1963)

Chao, K.C. and M. Lin, *"Synthesis gas solubility in Fischer-Tropsch slurry: Final report"*, Final Report for DOE Contract No. DE-AC22-84PC70024, DOE/PC/70024-T9, Purdue University, West Lafayette, IN, 1988

Deckwer W.-D., R. Kokuun, E. Sanders and S. Ledakowicz, *Ind. Eng. Chem. Process Des. Dev.*, 25, 643 (1986)

Dictor R.A. and A.T. Bell, *J. Catal*., 97:121–36 (1986)

Dry, M. E., T. Shingles, L. J. Boshoff and J. Oosthuizen, *J. Catal.*, 25, 99-104 (1972)

Edmister, W.C., *Pet. Refin*., 37, 173 (1958)

Englezos, P. and N. Kalogerakis, (2001) *"Applied parameter estimation for Chemical Engineers"*, New York: Mercel Dekker, Inc.

Feimer J.L., P.L. Silveston and RT. Huggins, *Ind. Eng. Chem. Prod. Res. Dev.*, 20, 609 (1981)

Froment G.F. and Bischoff K.B., (1990) *"Chemical Reactor Analysis And Design"*, Second Edition, New York: John Wiley & Sons, Inc.

Gao W., R.L. Robinson Jr. and K.A.M. Gasem, *J.Chem.Eng.Data*, 44, 130 (1999)

Gao W., R.L. Robinson, Jr. and K.A.M. Gasem, *Fluid Phase Equilibria*, 179, 207–216 (2001)

Gasem, K.A.M. and R.L. Robinson, Jr., *J.Chem.Eng.Data*, 30, 53 (1985)

Joback, K. G., *M.S. Thesis*, Massachusetts Institute of Technology, Cambridge, MA, June, 1984

Joback K.G. and R.C. Reid, *Chem. Eng. Comm*., 57, 233 (1987)

Klincewicz, K.M. and R.C. Reid, *AIChE*, 30 (1), 137 (1984)

Lee, B.I. and M.G. Kesler, *AIChE*, 21 (3), 510-527 (1975)

Li, Y.W. and Froment, G.F., *"ARSOFTS: Advanced Reactor Simulation of Fischer-Tropsch Synthesis"*, Unpublished work, Laboratorium voor Petrochemische Techniek, Rijksuniversiteit, Gent, Belgium, May, 1996

Lox, E. S. and G. F. Froment, *Ind. Eng. Chem. Res.*, 32, 61 (1993a)

Lox, E. S. and G. F. Froment, *Ind. Eng. Chem. Res.*, 32, 71 (1993b)

Lydersen, A.L., *"Estimation of Critical Properties of Organic Compounds", Univ. Wisconsin Coll. Eng., Eng. Exp. Stn. rept. 3*, Madison, WI, April, 1955
Marano, J.J. and G.D. Holder, *Fluid Phase Equilibrium*, 138, 1-21 (1997)
Marquardt, D.W., *J. Soc. Industr. Appl. Math.*, 11, 431 (1963)
Miller, S.A., and A. Ekstrom, *J. Chem. Eng. Data*, 35, 125 (1990)
Nikitin E.D., P.A. Pavlov and A.P. Popov, *Fluid Phase Equilib.*, 141, 155 (1997)
Nettelhoff, H., R. Kokuun, S. Ledakowicz and W.D. Decker, *Ger. Chem. Eng.*, 8, 177 (1985)
Park, J., and R.L. Robinson, Jr. and K.A.M. Gasem, *J.Chem.Eng.Data*, 40, 241 (1995)
Passut, C.A. and R.P. Danner, *Ind. Eng. Chem. Process Des. Develop.*, 12 (3) (1973)
Peng, D. Y. and D.B. Robinson, *Ind. Eng. Chem. Fundam.*, 15 (1), 59 (1976)
Peter, S. and M. Weinert, Z. Phys. Chem., (Neue Folge) 5, 114 (1955)
Poling, B.E., J.M. Prausnitz and J.P. O'Connell, (2001) *"The Properties of Gases and Liquids*", Fifth Edition, New York: McGraw-Hill
Reid, R.C., J.M. Prausnitz and T.K. Sherwood, (1977) *"The properties of gases and liquids*", Third Edition, New York: McGraw-Hill
Wang Y.-N., W.P. Maa, Y.J. Lua, J. Yangb, Y.Y. Xua, H.W. Xianga, Y.W. Lia, Y.L. Zhaoa and B.J. Zhang, *Fuel*, 82, 195-213 (2003)
Yang J., L. Ying, J. Chang, Y.N. Wang, L. Bai, Y.Y. Xu, H.W. Xiang, Y.W. Li and B. Zhong, *Ind. Eng. Chem. Res.*, 42, 21 (2003)
Zimmerman, W. H. and D. B. Bukur, *Can. J. Chem. Eng.*, 68, 292 (1990)
Zimmerman, W. H., *"Kinetic Modeling of the Fischer-Tropsch Synthesis"*, Ph.D. dissertation, Texas A&M University, College Station, TX, 1990
Zimmerman, W., D.B. Bukur and S. Ledakowicz, *Chem. Eng. Sci.*, 47, 2707 (1992)

Table 1. Mass balances used for VLE calculations and kinetic parameter estimation.

	MB#	TOS	T	P	H_2/CO	SV
		h	°C	bar	(-)	NL/g-Fe/h
SB-21903	I/1	71-78	260	15	0.67	4.0
	I/2	94-101	260	15	0.67	1.7
	I/3	119-126	260	15	0.67	9.2
	I/4	152-164	240	15	0.67	2.0
	I/5	193-215	240	15	0.67	1.0
	I/6	225-238	240	15	0.67	5.5
	I/7	263-270	260	15	0.67	4.0
	I/8	298-310	240	15	2	4.2
	I/10	364-368	240	15	2	10.8
	I/13	489-505	260	15	0.67	4.0
	I/14	600-606	260	22.5	0.67	6.1
	I/15	647-654	260	22.5	0.67	1.0
SB-26203	II/1	86-92	260	15	2	7.1
	II/2	118-122	260	15	2	10.1
	II/3	142-146	260	15	2	23.5
	II/4	175-191	240	15	2	5.8
	II/5	224-240	260	25	0.67	6.7
	II/6	264-268	260	25	0.67	17.1
	II/7	297-313	260	25	0.67	2.0
SB-28603	III/1	94-101	220	15	0.67	4.1
	III/2	128-143	220	15	0.67	0.5
	III/3	166-170	220	15	2	9.5
	III/4	192-198	220	15	2	0.6
	III/5	224-238	260	8	2	1.5
	III/6	262-268	260	8	2	9.0
	III/7	287-292	240	8	0.67	5.5
	III/8	313-318	240	8	0.67	0.7

Table 2. Solubility data for inorganic species in hydrocarbons.

Authors	Solute	Solvent			T	P
		Name	CN	MW		
				g/mol	°C	bar
Chao and Lin, 1988	Hydrogen, Carbon Monoxide, Carbon Dioxide, Syngas	n-Eicosane	20	282	100 – 300	10 – 50
		n-Octacosane	28	394		
		n-Hexatriacontane	36	506		
		Mobil Wax	?	?		
		Sasol Wax	?	?		
Breman *et al*., 1994	Hydrogen,	n-Hexadecane, n-Octacosane	28	394	150 - 250	40 - 50
	Carbon Monoxide					30 - 38
	Carbon Dioxide					20 - 25
	Water					1.5 - 2.5
Peter and Weinert, 1955	Hydrogen*, Carbon Monoxide, Carbon Dioxide, Water	Wax 250	~18	250	106 - 300	1 – 100
		Wax 345	~24.5	345		
Gasem and Robinson, 1985; Park *et al*., 1995; Gao *et al*., 1999	Hydrogen, Carbon Dioxide	n-Decane	10	142	100, 150	10 - 50
		n-Eicosane	20	282		
		n-Octacosane	28	394		
		n-Hexatriacontane	36	506		
	Carbon Monoxide	n-Dodecane	12	170		
	Carbon Dioxide	n-Tetratetracontane	44	619		
Calderbank *et al*., 1963	Hydrogen	Krupp Wax			107 - 300	1
Nettelhoff *et al*., 1985	Hydrogen, Carbon Monoxide	Vestowax	28	394	200 – 240	4 - 12
Miller and Ekstrom, 1990	Hydrogen, Carbon Monoxide	n-Octacosane, Gulf, FT-heavy, Mobil FT	28 ? ? ?	394 ? ? ?	~250	?

? – No information provided by authors.

Table 3. Estimated values of binary interaction coefficients k_{ij} in Peng-Robinson EOS.

Solvent		**Solute**			
CN	**Name**	**Hydrogen**	**Carbon Monoxide**	**Carbon Dioxide**	**Water**
10	n-Decane	0.2852	-	-	-
16	n-Hexadecane	-	-	-	0.3008
20	n-Eicosane	0.3233	0.2108	0.0878	-
~25	wax 345 g/mol	-	-	-	0.2098
28	n-Octacosane	0.4071	0.1878	0.0477	0.0542
36	n-Hexatriacontane	1.0496	0.4976	0.0679	-

Table 4. Elementary reactions for FTS (ALII Model in Lox and Froment, 1993b).

No.	Elementary reactions	Expression of rates (small) and equilibrium constants (capital letter)
HC1	$CO + C_{n-1}H_{2n-1}l_1 \rightarrow C_{n-1}H_{2n-1}\,l_1CO$ $n \geq 1$	$k_{HC1}\ (k_{CO})$
HC 2	$C_{n-1}H_{2n-1}\,l_1CO + H_2 = C_{n-1}H_{2n-1}\,l_1C + H_2O$ $n \geq 1$	K_{HC2}
HC 3	$C_{n-1}H_{2n-1}\,l_1C + H_2 = C_{n-1}H_{2n-1}\,l_1CH_2$ $n \geq 1$	K_{HC3}
HC 4	$C_{n-1}H_{2n-1}\,l_1CH_2 = C_nH_{2n+1}l_1$ $n \geq 1$	K_{HC4}
HC 5	$C_nH_{2n+1}\,l_1 + H_2 \rightarrow C_nH_{2n+2} + Hl_1$ $n \geq 1$	$k_{\mathrm{HC5}}\ (k_{\mathrm{t,p}})$
HC 6	$C_nH_{2n+1}\,l_1 \rightarrow C_nH_{2n} + Hl_1$ $n \geq 2$	$k_{\mathrm{HC6}}\ (k_{\mathrm{t,o}})$
HC 7	$H_2 + 2l_1 = 2Hl_1$	$K_{\mathrm{HC7}}\ (K_{\mathrm{H_2}})$

where l_1 is a vacant active site on the surface of catalyst.

Table 5. Elementary reactions for WGS (ALII Model in Lox and Froment, 1993b).

No.	Elementary reactions	Expression of rates (small) and equilibrium constants (capital letter)
WGS1	$CO + l_2 = COl_2$	$K_{1,WGS}$
WGS2	$COl_2 + OHl_2 = COOHl_2 + l_2$	$k_{2,WGS}$, $K_{2,WGS}$
WGS3	$COOHl_2 = CO_2 + Hl_2$	$K_{3,WGS}$
WGS4	$H_2O + 2 \cdot l_2 = OHl_2 + Hl_2$	$K_{4,WGS}$
WGS5	$H_2 + 2 \cdot l_2 = 2 \cdot Hl_2$	$K_{5,WGS}$

where l_2 is a vacant active site on the surface of catalyst, but different type than l_1 (in Table 4)

Table 6. Estimated values of kinetic parameters (ALII Model of Lox and Froment).

Parameter	**units**	**220°C**	**240°C**	**260°C**
(a) Weighting factors equal to 1				
$k_{CO,HC}$	mmol/kg/s/bar	0.277	1.46	4.02
$k_{t,p}$	mmol/kg/s/bar	0.151	0.0352	0.131
$k_{t,o}$	mmol/kg/s	-0.618	0.00644	-0.166
$k_{\nu}^{'}$	mmol/kg/s/bar^1.5	8.04	0.817	25.2
K_{ν}	bar^-0.5	23.6	0.7	9.35
(b) Weighting factors from equation (25)				
$k_{CO,HC}$	mmol/kg/s/bar	0.0709	0.39	1.55
$k_{t,p}$	mmol/kg/s/bar	0.00463	0.016	0.0434
$k_{t,o}$	mmol/kg/s	0.0194	0.031	0.051
$k_{\nu}^{'}$	mmol/kg/s/bar^1.5	0.194	0.53	9.08
K_{ν}	bar^-0.5	1.31	0.533	7.05

Table 7. Confidence intervals for kinetic parameters (ALII Model of Lox and Froment).

T = 220 °C	***units***	***Parameter estimate***	***95%-confidence limit***	
			lower	***upper***
$k_{CO,HC}$	mmol/kg/s/bar	0.0709	0.0561	0.0856
$k_{t,p}$	mmol/kg/s/bar	0.00463	0.00365	0.00562
$k_{t,o}$	mmol/kg/s	0.0194	0.0143	0.0245
$k_{\nu}^{'}$	mmol/kg/s/bar^1.5	0.194	-0.401	0.79
K_{ν}	bar^-0.5	1.31	-4.34	6.97

T = 240 °C	***units***	***Parameter estimate***	***95%-confidence limit***	
			lower	***upper***
$k_{CO,HC}$	mmol/kg/s/bar	0.391	0.324	0.459
$k_{t,p}$	mmol/kg/s/bar	0.016	0.0138	0.0182
$k_{t,o}$	mmol/kg/s	0.0305	0.023	0.038
$k_{\nu}^{'}$	mmol/kg/s/bar^1.5	0.531	-1.06	2.12
K_{ν}	bar^-0.5	0.533	-4.2	5.27

T = 260 °C	***units***	***Parameter estimate***	***95%-confidence limit***	
			lower	***upper***
$k_{CO,HC}$	mmol/kg/s/bar	1.55	1.28	1.81
$k_{t,p}$	mmol/kg/s/bar	0.0434	0.0384	0.0484
$k_{t,o}$	mmol/kg/s	0.051	0.0286	0.0733
$k_{\nu}^{'}$	mmol/kg/s/bar^1.5	9.08	-43.8	62
K_{ν}	bar^-0.5	7.05	-20.1	34.2

Table 8. Activation energies and statistical parameters for the FTS and WGS reactions.

Units (kJ/mol)		*Standard Error*	*t Stat*	*Lower 95%*	*Upper 95%*
$E_{CO,HC}$	168.73	6.62	25.49	84.62	252.85
$E_{t,p}$	122.41	4.89	25.05	60.33	184.50
$E_{t,o}$	52.75	3.13	16.84	12.96	92.55
E_{ν}	208.78	62.51	3.34	-585.46	1003.02

Table 9. Activation energies for the FTS and WGS reactions from the literature (in kJ/mol)

Author(s), Year	**Reactor**	**Catalyst**	**Paraffin formation**	**Olefin formation**	**WGS**	**Overall FT**
Yang *et al*., 2003	Fixed bed	Fe/Mn	97 – methane 111 – C_2^+	97	58	
Wang *et al*., 2003	Fixed bed	Fe/Cu/K	93 – methane 87 – C_2^+	111	45	
Lox and Froment, 1993	Fixed bed	Fe	94	132	28	
Zimmerman and Bukur, 1990	Slurry	Fe/Cu/K			132 – 137	86
Deckwer *et al*., 1986	Slurry	Fe/K			63 – 105	
Dictor and Bell, 1986	Slurry	Reduced and Unreduced Fe and Fe/K	80 – 90*	100 – 110*		105 (Fe/K), 109 (Fe)
Feimer *et al*., 1981	Fixed bed	Fe/Cu/K_2O	92 – CH_4 84 – C_2H_6 78 (C_2 – C_5 HC)		124	
Dry *et al*., 1972	Fixed bed differential	Fe/K_2O/Al_2O_3/SiO_2	70 (C_2 – C_5 HC **)			70

*as reported by Yang *et al*., 2003
**as reported by Feimer *et al*., 1981

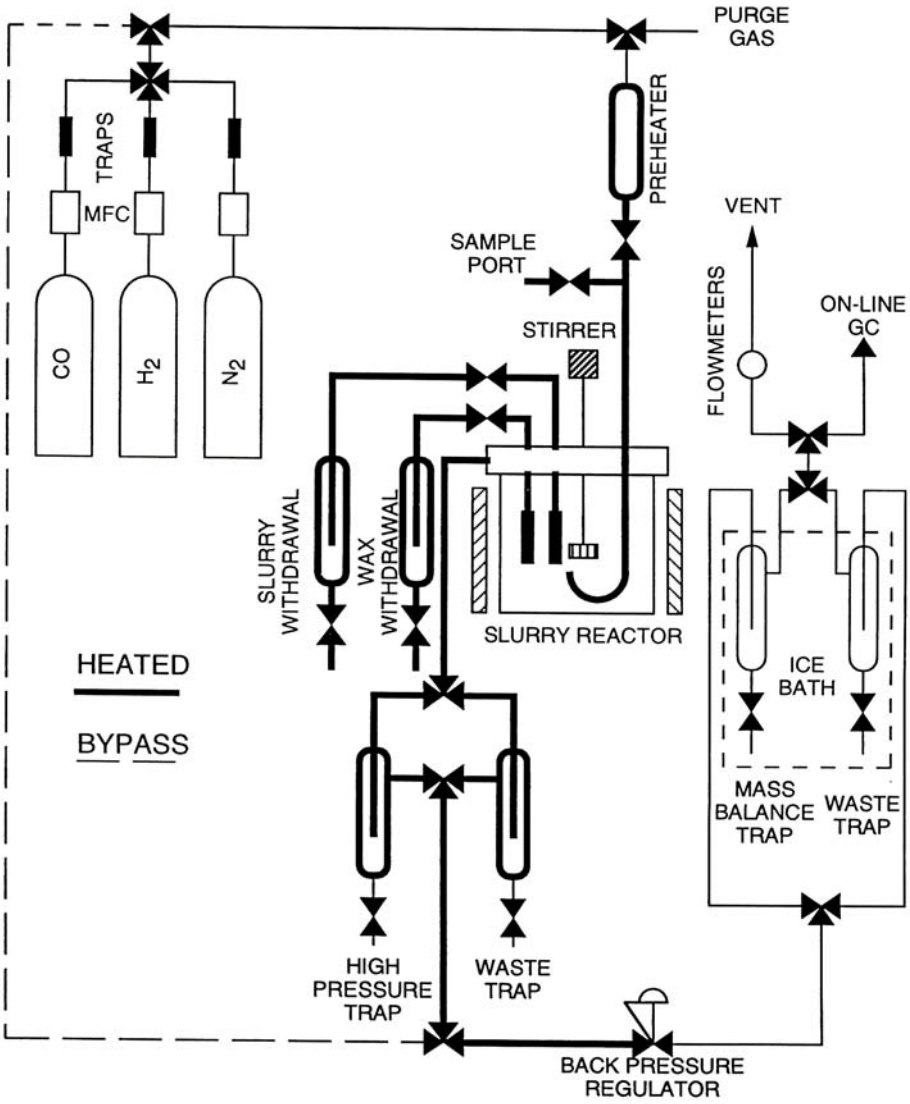

Figure 1. Schematic of stirred tank slurry reactor system.

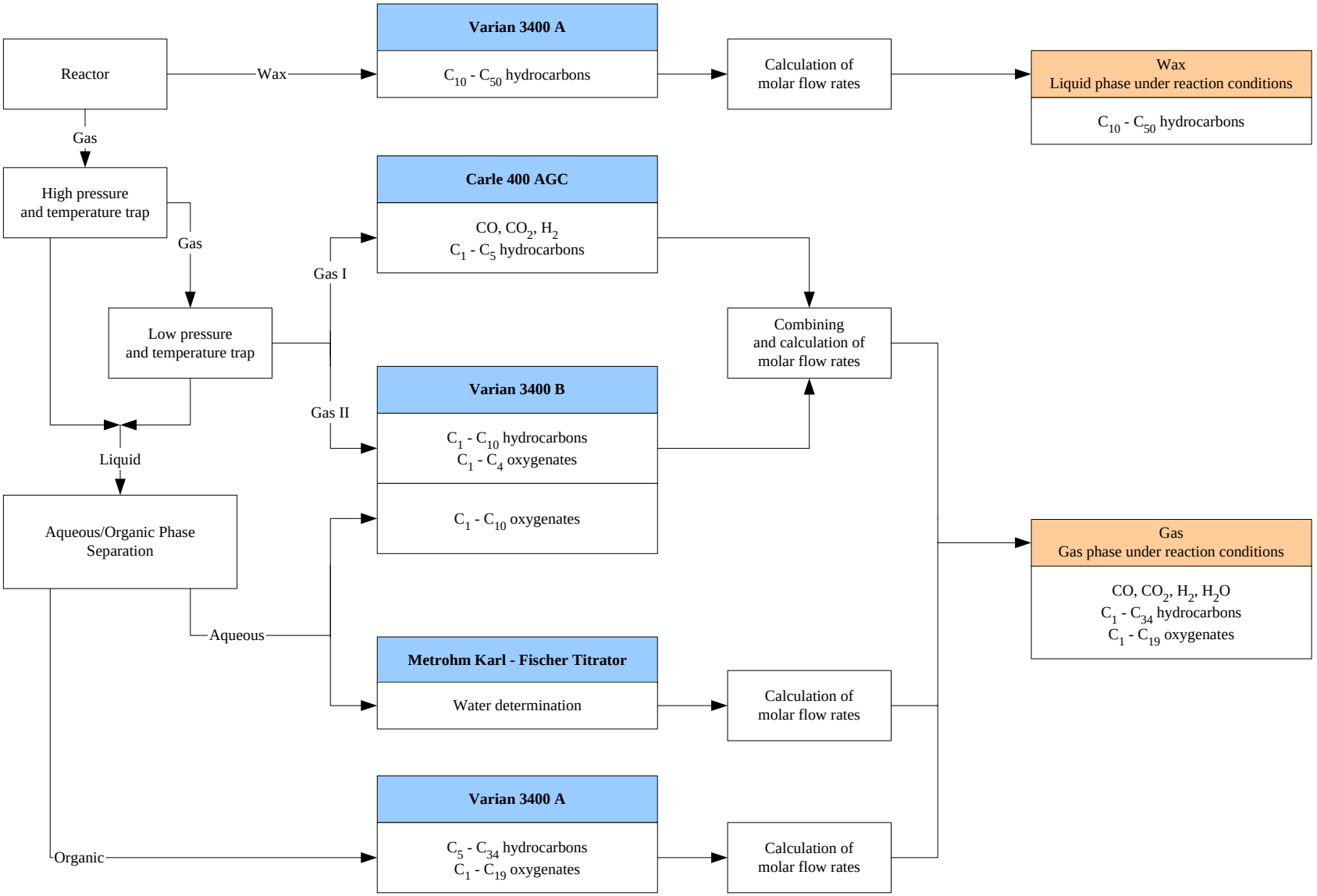

Figure 2. Product analysis schematic.

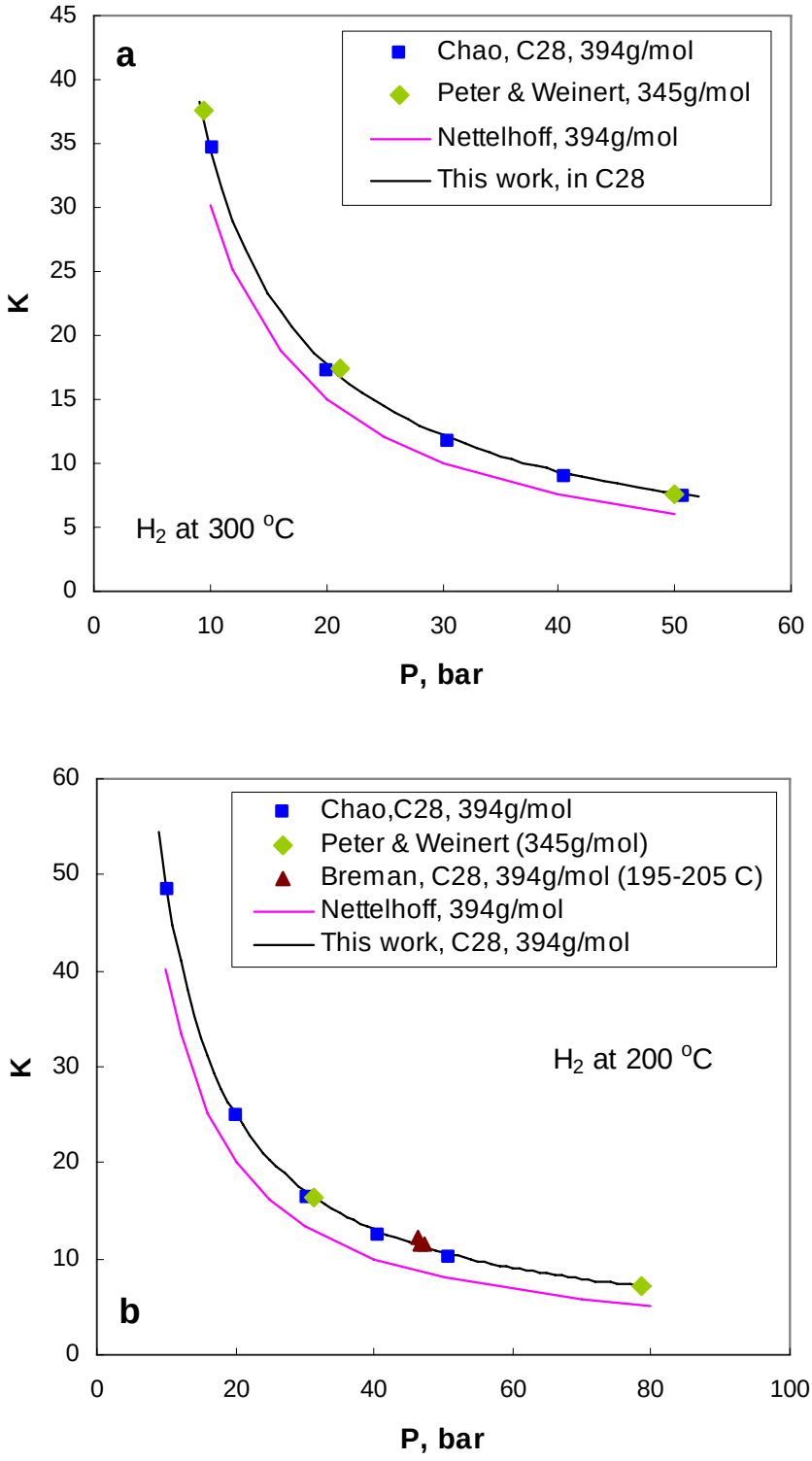

Figure 3. VLE calculations for binary system:
hydrogen in n-Octacosane ($C_{28}H_{58}$, MW = 394 g/mol).

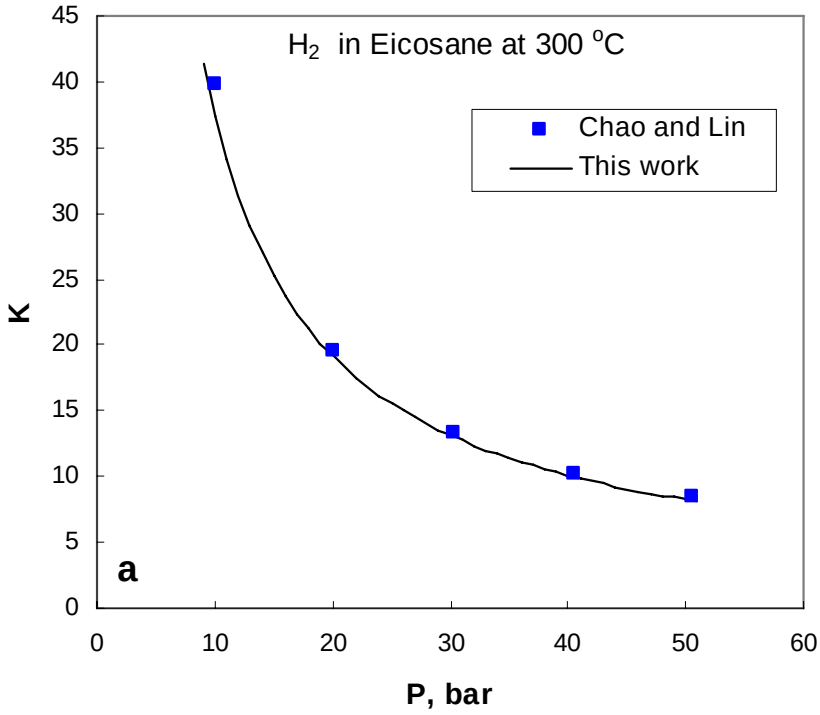

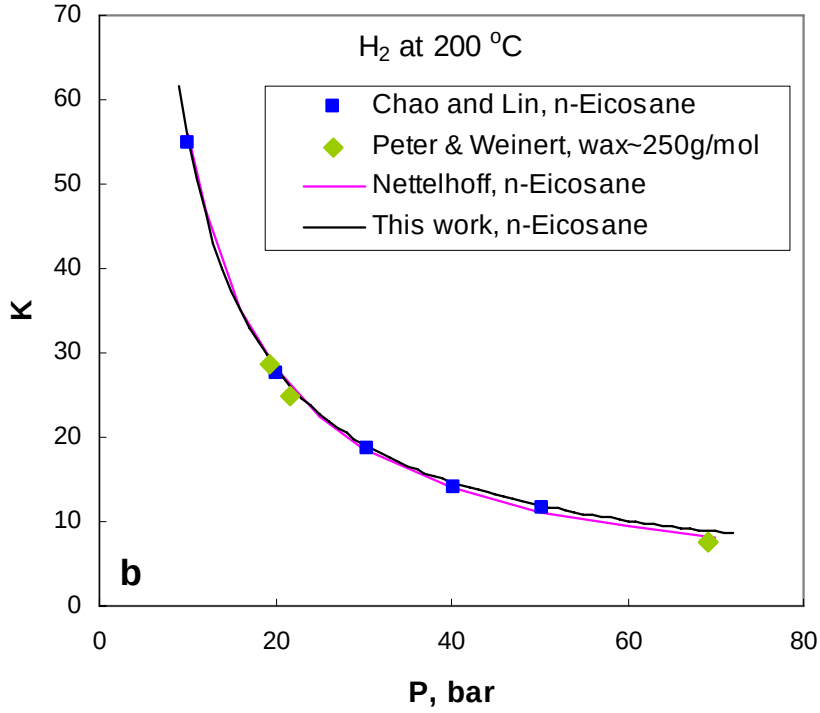

Figure 4. VLE calculations for binary system:
hydrogen in n-Eicosane ($C_{20}H_{42}$, MW = 282 g/mol).

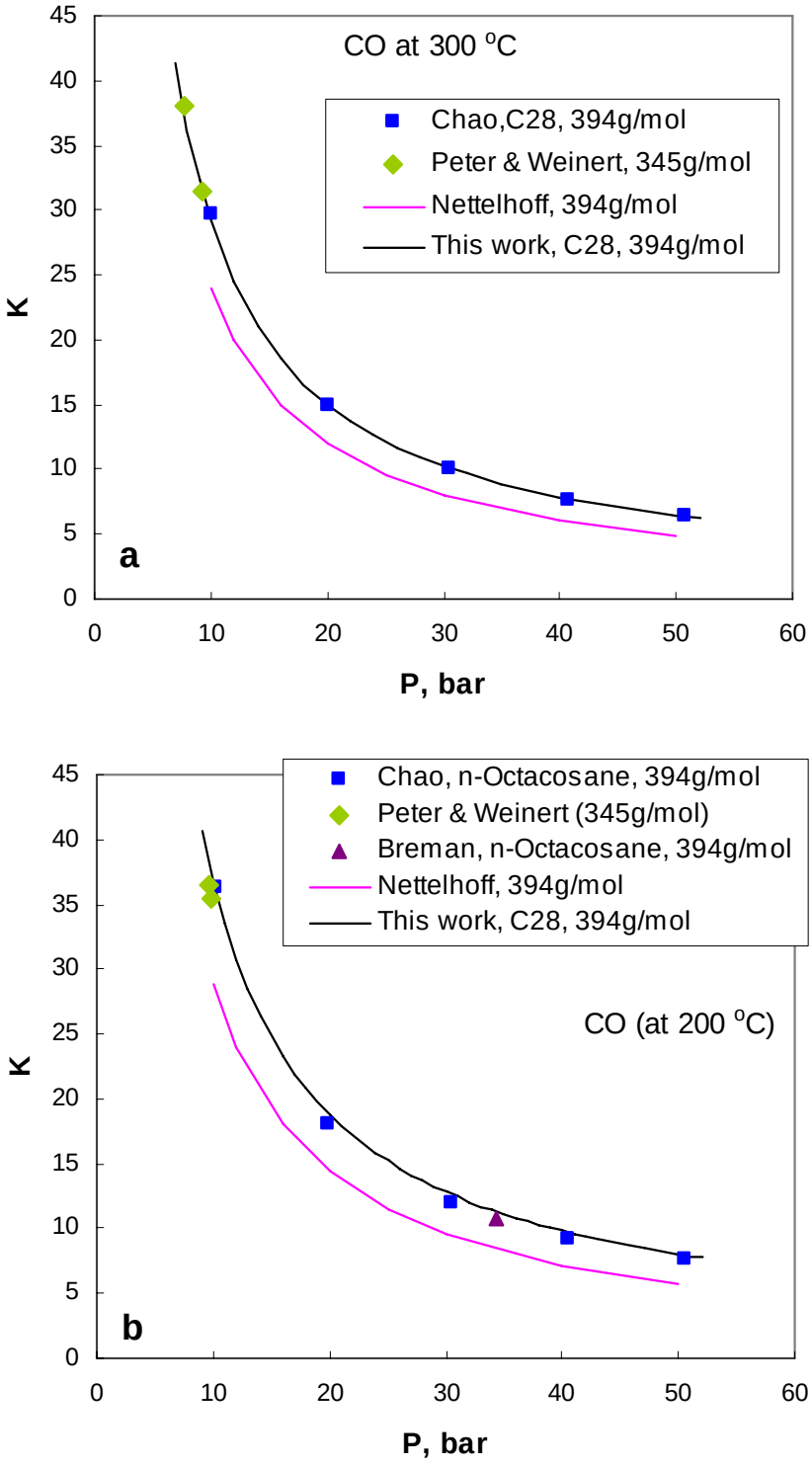

Figure 5. VLE calculations for binary system:
carbon monoxide in n-Octacosane ($C_{28}H_{58}$, MW = 394 g/mol).

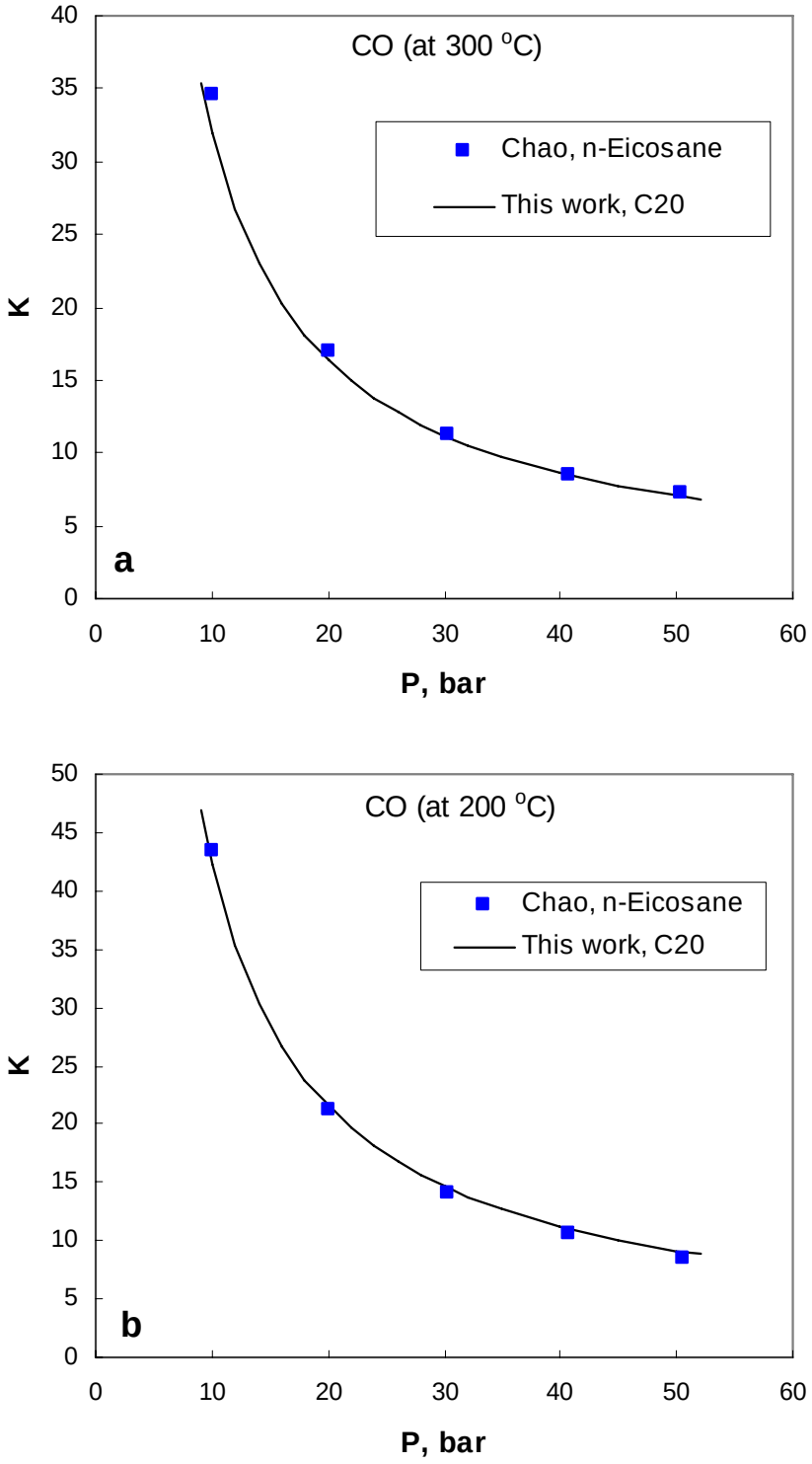

Figure 6. VLE calculations for binary system:
carbon dioxide in n-Eicosane ($C_{20}H_{42}$, MW = 282 g/mol).

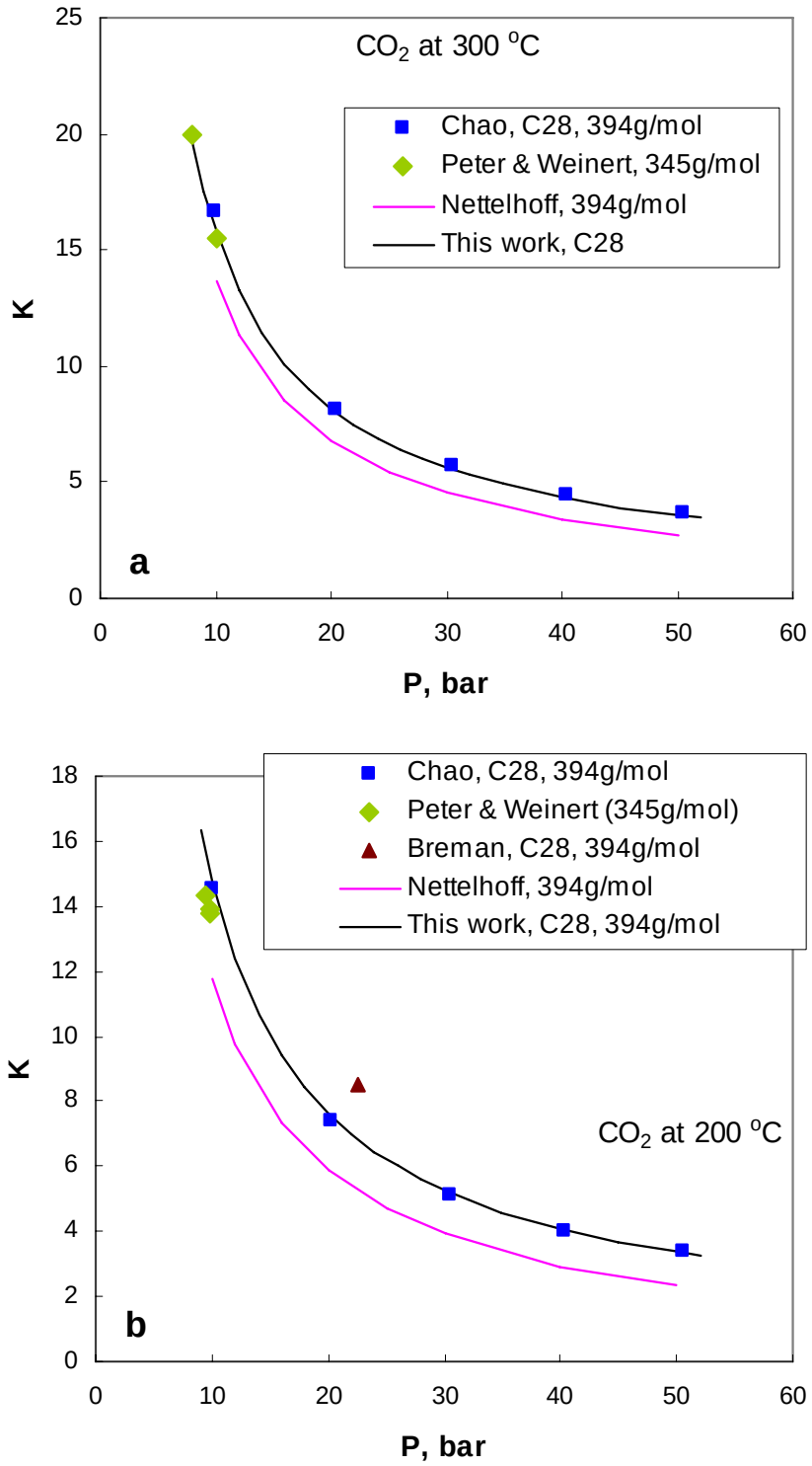

Figure 7. VLE calculations for binary system:

carbon dioxide in n-Octacosane ($C_{28}H_{58}$, MW = 394 g/mol).

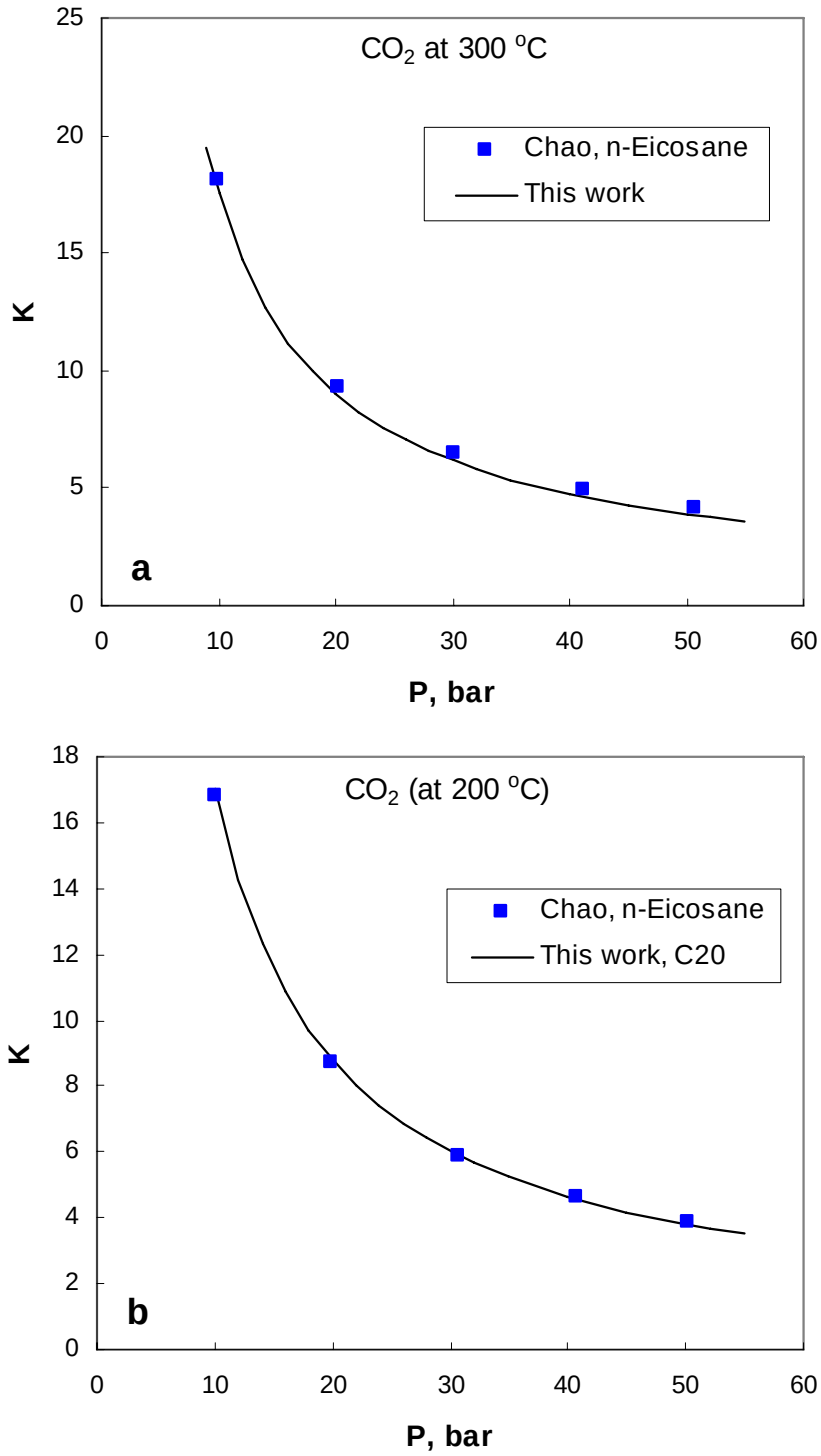

Figure 8. VLE calculations for binary system:
carbon monoxide in n-Eicosane ($C_{20}H_{42}$, MW = 282 g/mol).

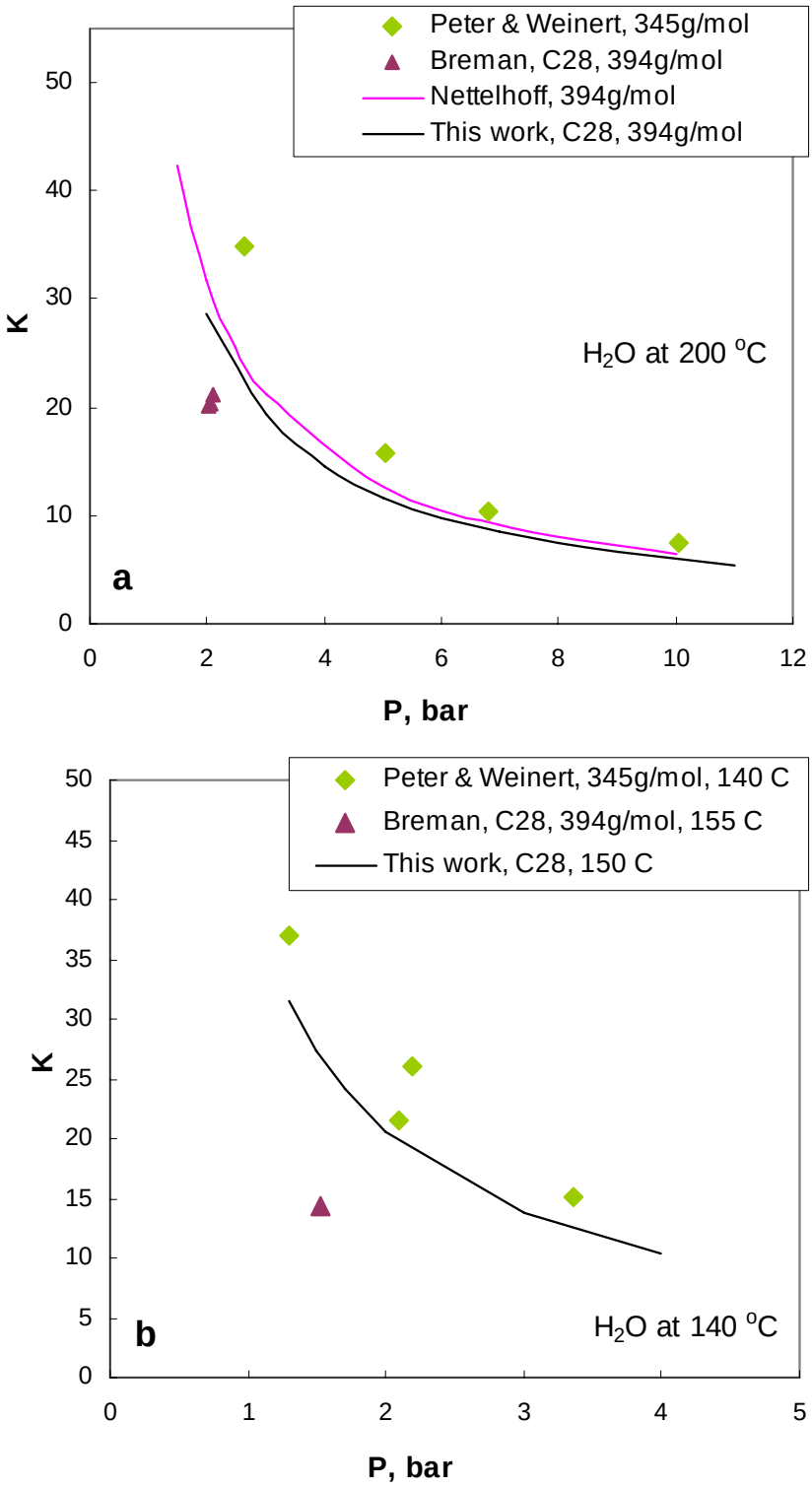

Figure 9. VLE calculations for binary system:
water in n-Octacosane ($C_{28}H_{58}$, MW = 394 g/mol).

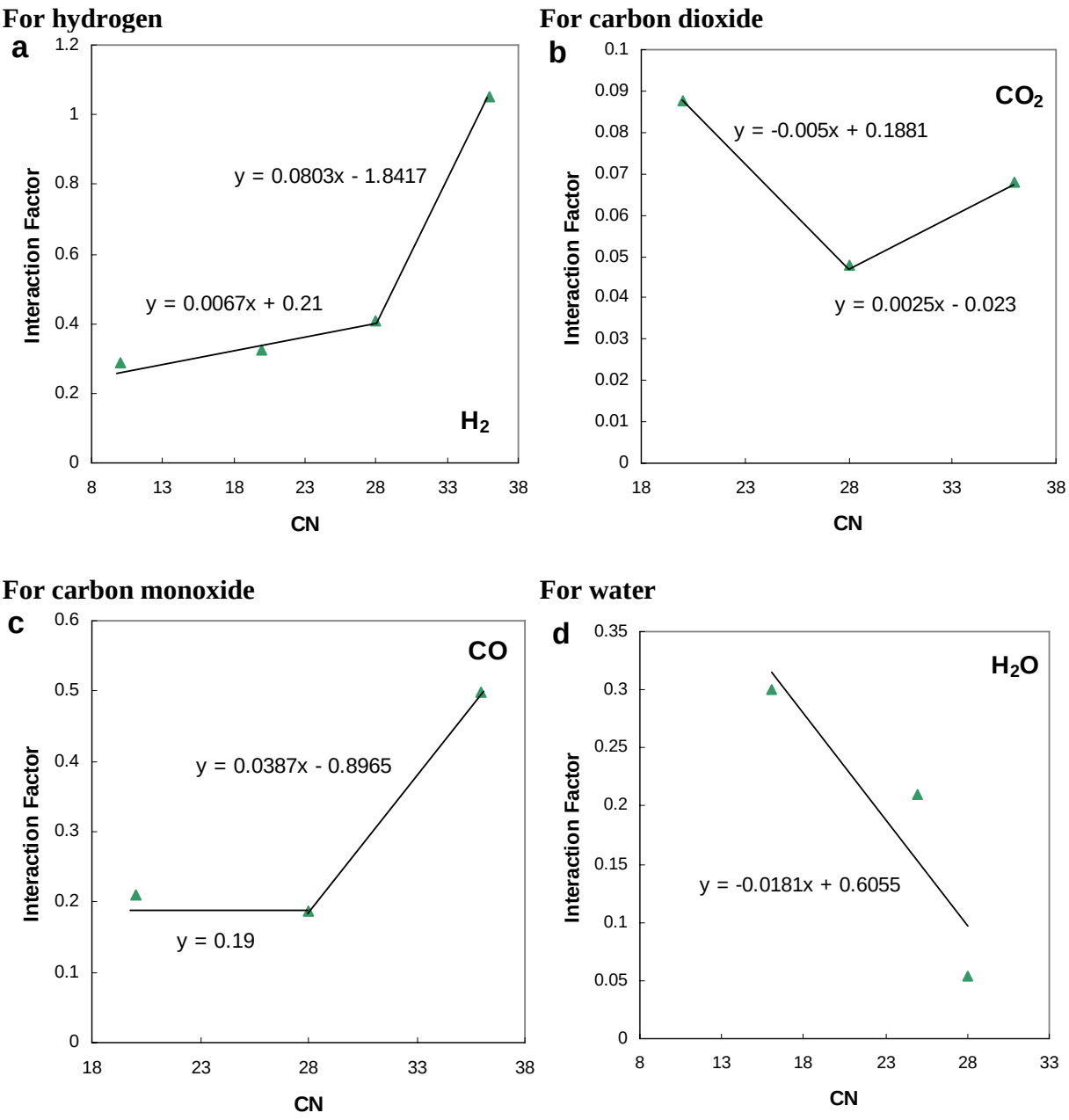

Figure 10. Estimated k_{ij} interaction factors as a function of carbon number.

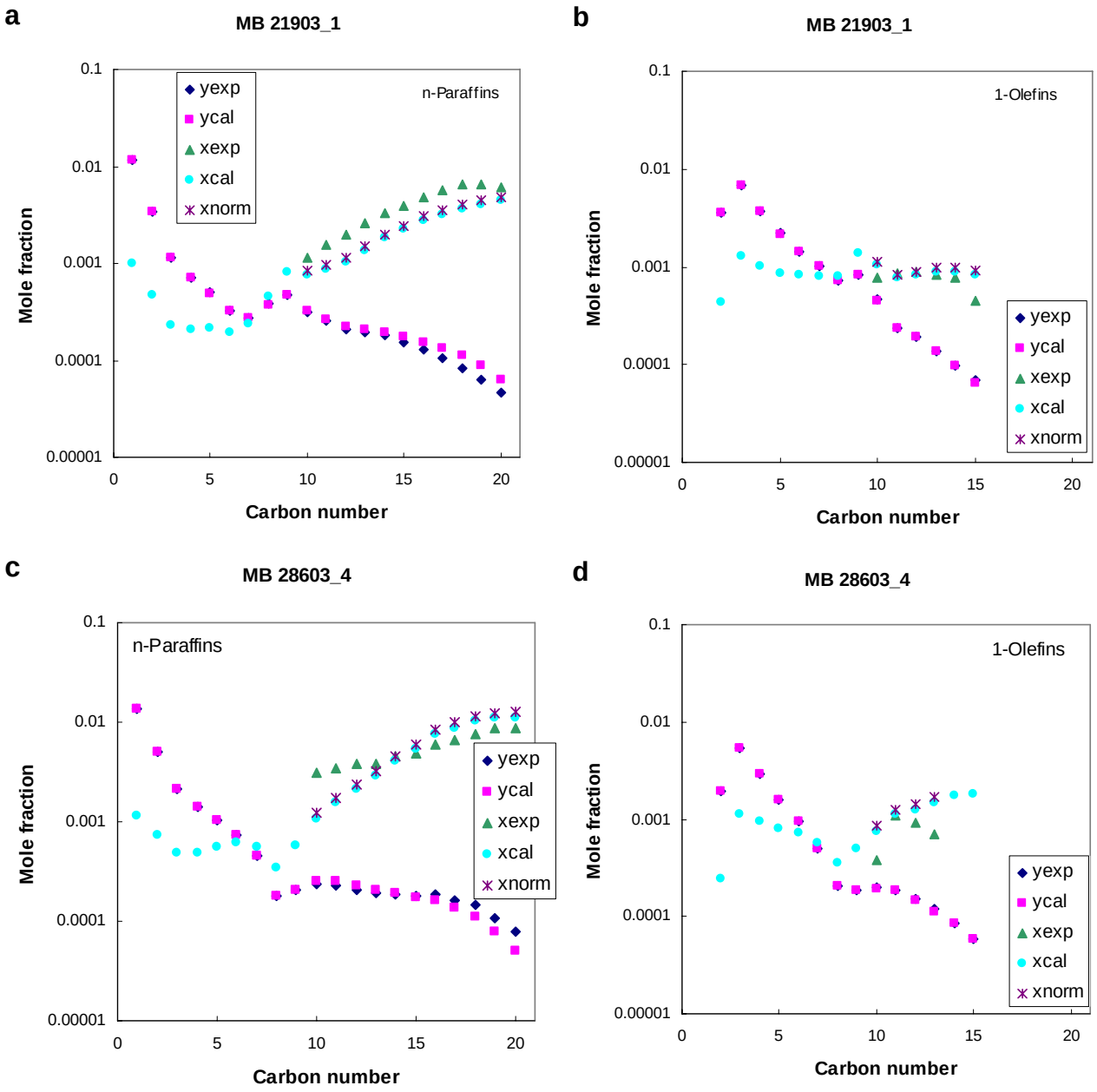

Figure 11. VLE calculations for FTS in the STSR. Reaction conditions: MB 21903_15 (a and b): 260°C, 2.17 bar, 0.68 H_2/CO and SV = 1.4 Nl/g_{Fe}/h; MB 28603_4 (c and d): 220°C, 1.48 bar, 2 H_2/CO and SV = 0.55 Nl/g_{Fe}/h.

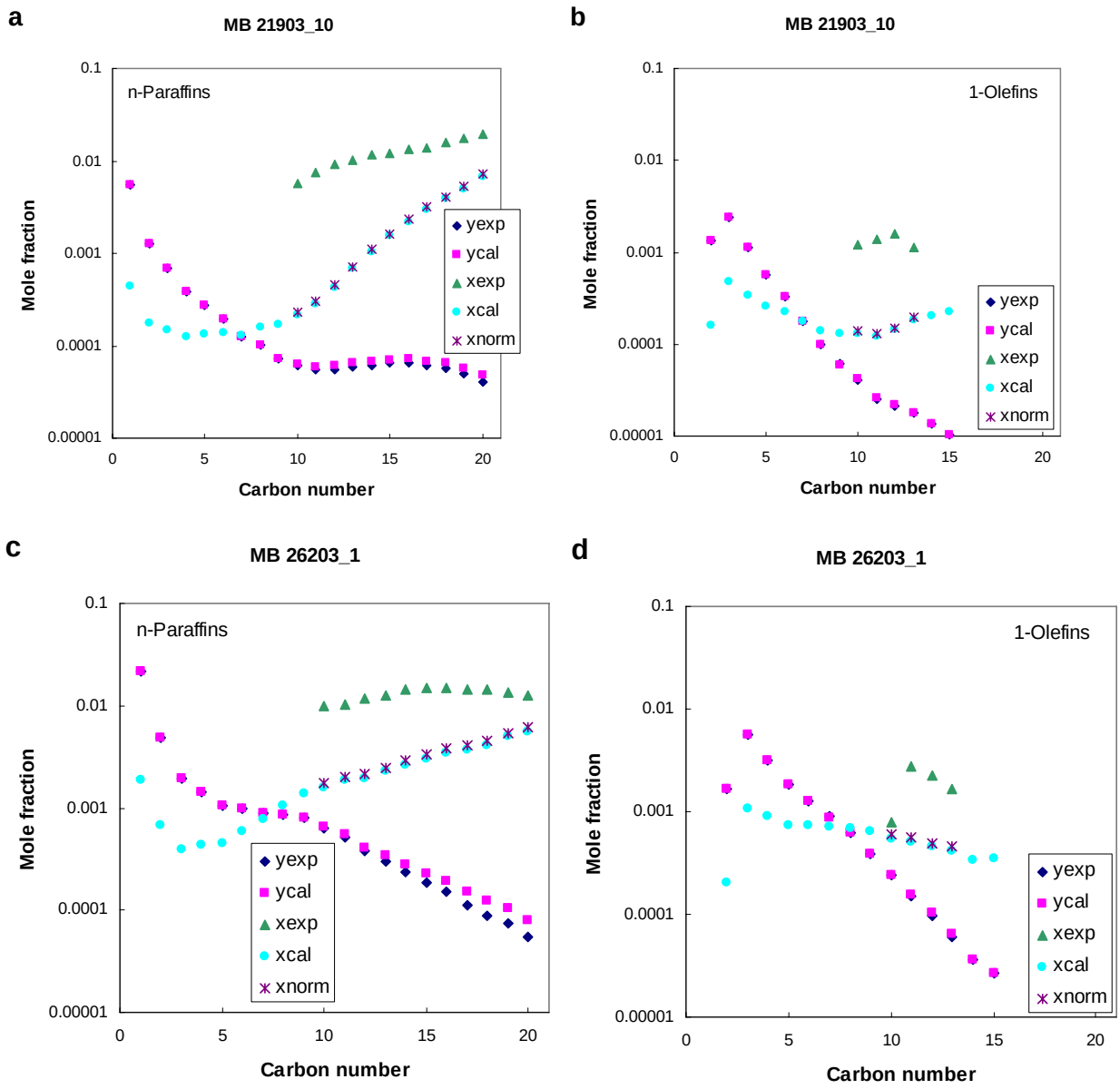

Figure 12. VLE calculations for FTS in the STSR. Reaction conditions: MB 21903_10 (a and b): 240°C, 1.48 bar, 2 H_2/CO and SV = 10.8 Nl/g_{Fe}/h; MB 26203_1 (c and d): 260°C, 1.48 bar, 2 H_2/CO and SV = 7.1 Nl/g_{Fe}/h.

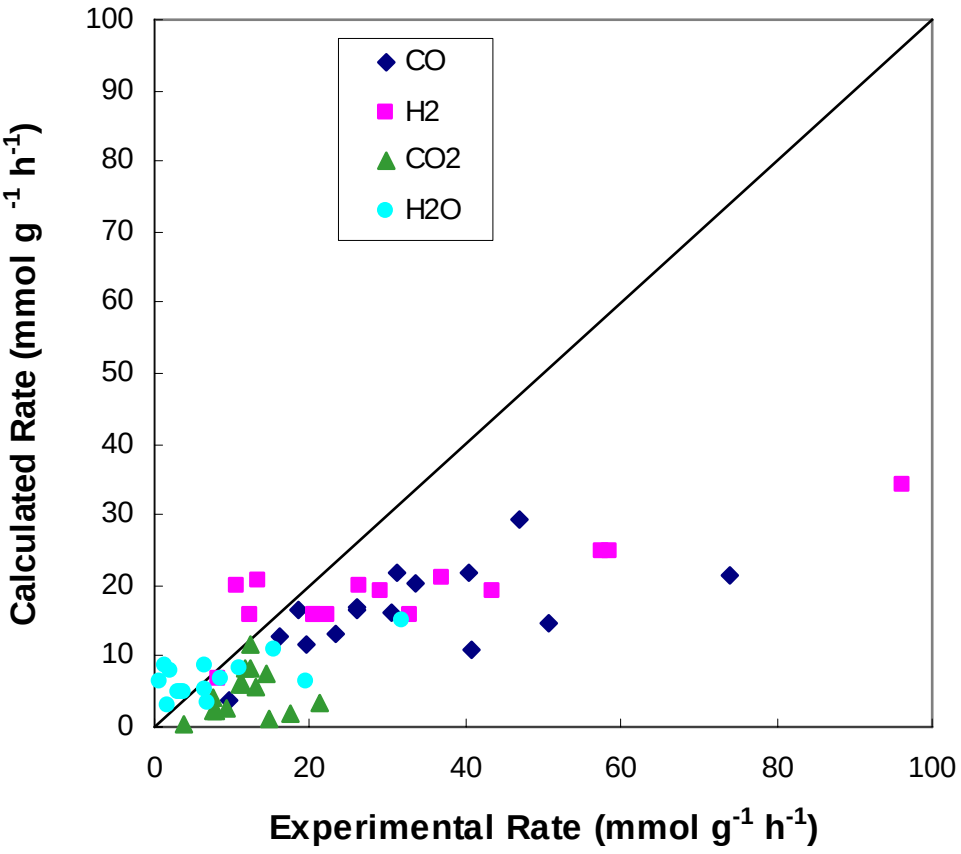

Figure 13. Parity graph of experimental and calculated reaction rates at *260 ℃* for H_2, CO, CO_2 and H_2O.

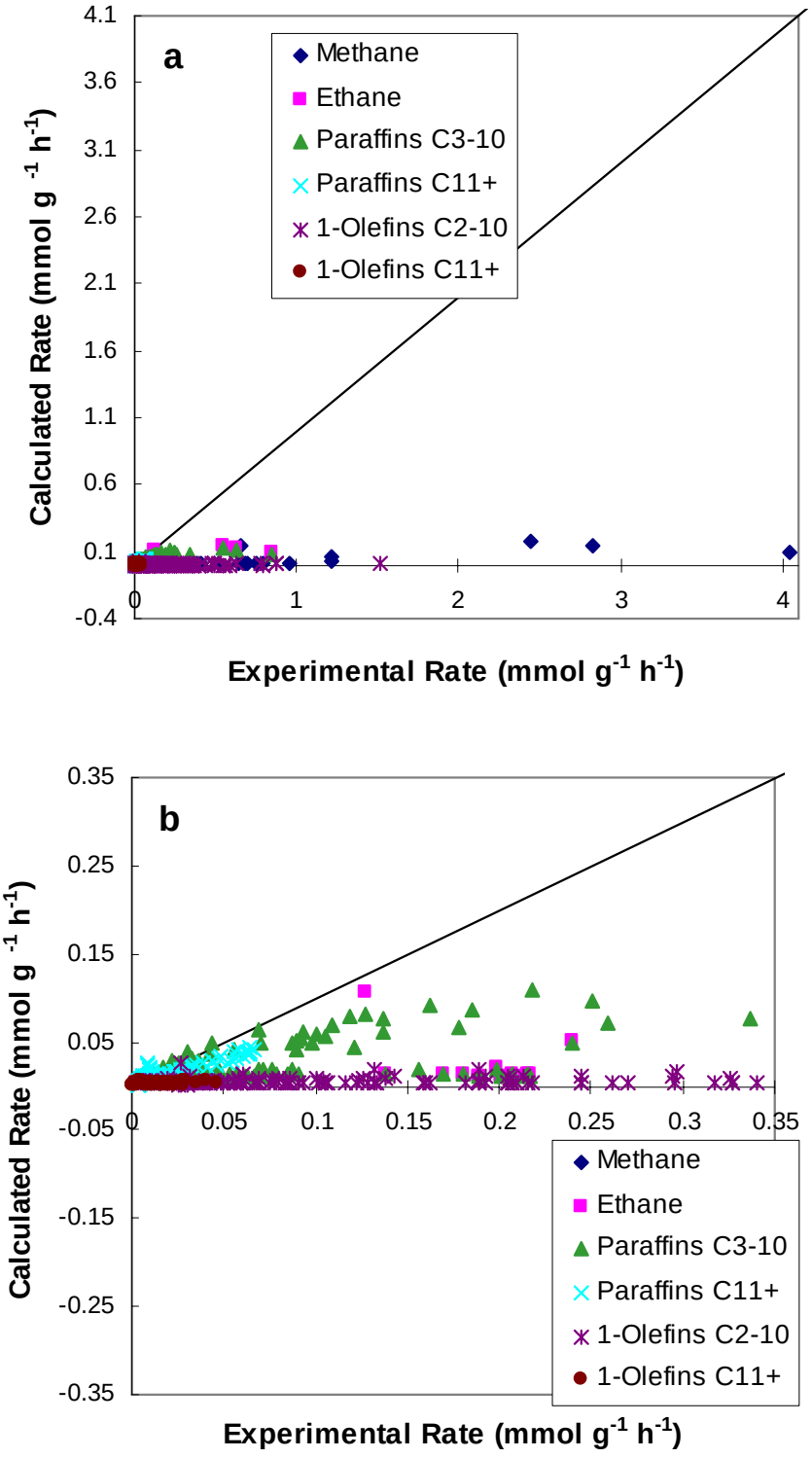

Figure 14. Parity graph of experimental and calculated reaction rates at *260 ℃* for hydrocarbons.

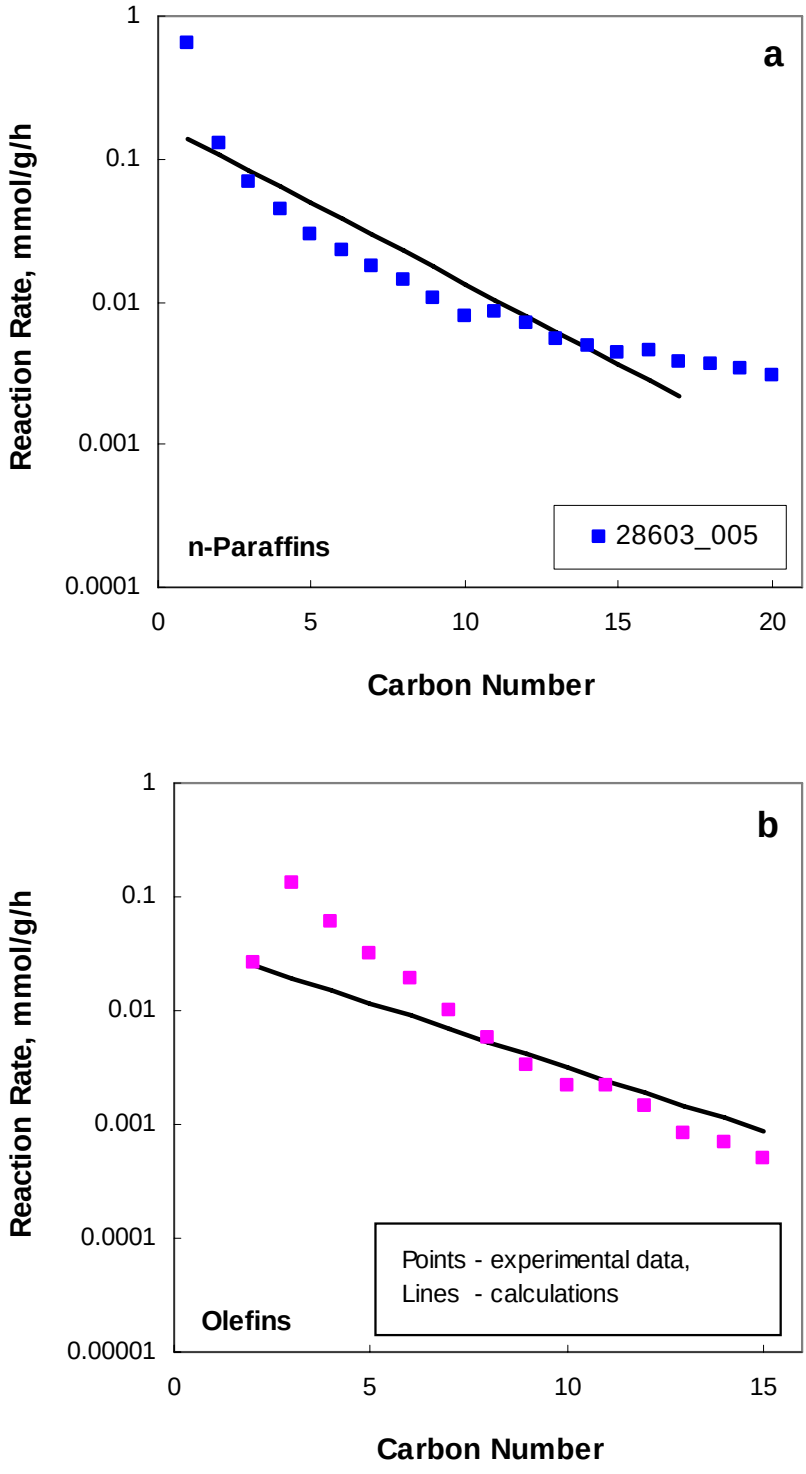

Figure 15. Comparison of experimental data and model predictions for n-paraffins and total olefins at T = 260°C, 8 bar, $H_2/CO = 2$, SV = 1.45 Nl/g_{Fe}/h).

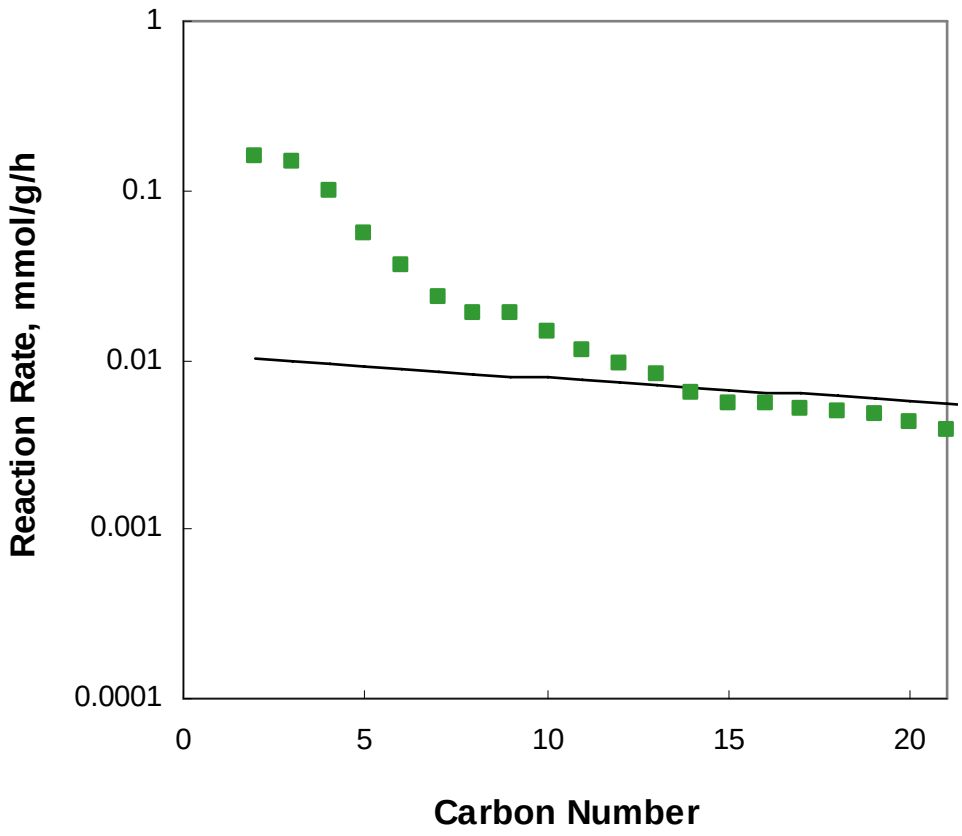

Figure 16. Carbon number distribution of hydrocarbon products - Comparison of model predictions with experimental data (Reaction conditions: T = 240°C, 15 bar, H_2/CO = 2/3, SV = 2.0 $Nl/g_{Fe}/h$).

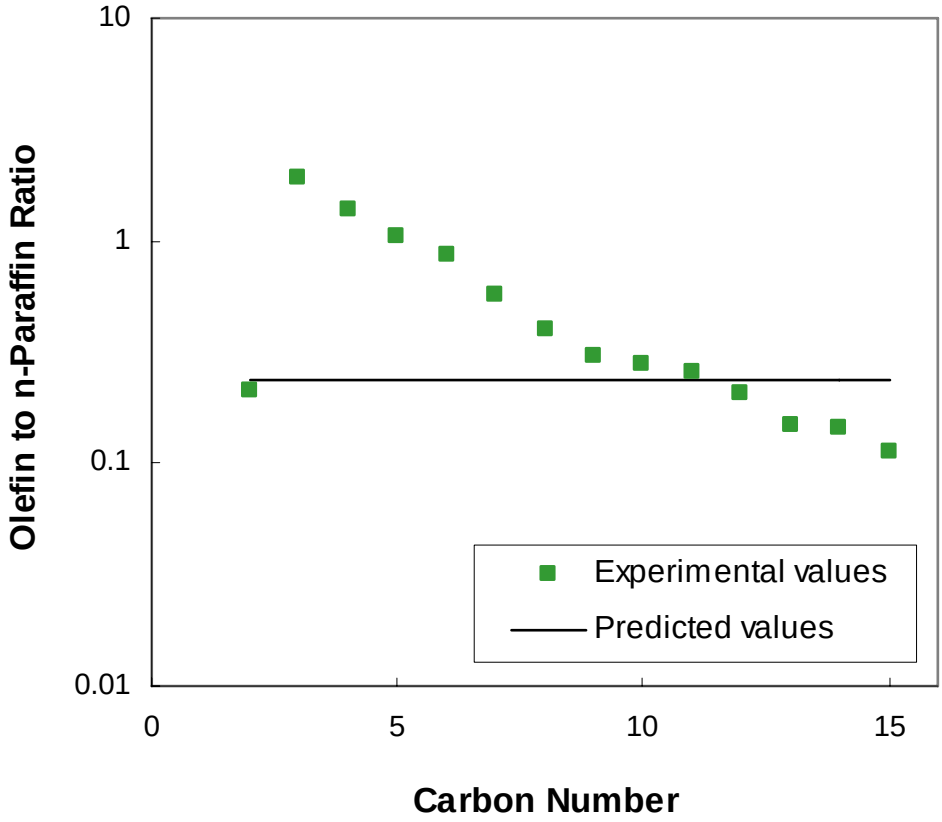

Figure 17. Olefin to paraffin ratio change with carbon number – Comparison of model predictions with experimental data (Reaction conditions: T = 260°C, 8 bar, $H_2/CO = 2$, SV = 1.45 $Nl/g_{Fe}/h$).

Notation

A - constant defined by eqn A.12

a - attraction parameter in equation of state (eqn. A.1)

a_i - mixing rules parameter defined by eqn. A.4

$a_{c,i}$ - mixing rules parameter defined by eqn. A.5

a_{ij} - mixing rules parameter defined by eqn. A.3

B - constant defined by eqn A.13

b - van der Waals co-volume parameter in equation of state (eqn. A.1)

b_i - mixing rules parameter defined by eqn. A.7

C_{l_i} - molar concentration of vacant active sites on the surface of catalyst per gram of catalyst, where *i* is 1 for FTS and 2 for WGS, *mol* g_{cat}^{-1}

$C_{l_i,tot}$ - total molar concentrations of the active sites of type l_1 (*i=1*) or l_2 (*i=2*) on the surface of the catalyst per gram of catalyst, *mol* g_{cat}^{-1}

C_j - molar concentrations of adsorbed *j* species on the surface of catalyst per gram of catalyst, *mol* g_{cat}^{-1}

F_i - molar flow rate of *i* component, *mol* h^{-1}

$\hat{f}_i$ - fugacity of a species *i* in solution, *Pa*

$f_i(\varpi)$ - function of acentric factor ω

K_i - K-value, vapor-liquid equilibrium constant characteristic for each species *i*

k_j - reaction rate constant (kinetic parameter), *units vary*

$k_{i,j}$ - binary interaction factor between two species

MW - molecular weight, *g* mol^{-1}

N_{atoms} - total number of atoms in Durasyn molecule

N_k - group number

n - number of isothermal experiments

n_e - number of replicate experiments

p_i - partial pressure, *Pa*

P - pressure, *Pa*

pck - group contribution parameter in eqn. B.1

SV - space velocity, $NL/g_{Fe}/h$

R - universal gas constant, $J\ mol^{-1}\ K^{-1}$

T - absolute temperature, *K*

T_b - boiling point, *K*

$T_{c,i}$ - critical temperature for pure *i* component, *K*

tck - group contribution parameter in eqn. B.2

$T_{r,i}$ - reduced temperature for pure *i* component, *K*

$P_{c,i}$ - critical pressure for pure *i* component, *Pa*

u_i - mole fraction of *i* species in the liquid x or in the gas y

v - number of components

x_i - mole fraction of species *i* in the liquid phase

xcal - calculated from VLE calculation mole fraction in the liquid phase

xexp - calculated from experimental analysis mole fraction in the liquid phase

xnorm - normalized calculated from experimental analysis mole fraction in the liquid phase (eqn. 5)

x_T - mole fraction of liquid phase in a total flux at the reactor exit

y_i - mole fraction of species *i* in the gas phase

ycal - calculated from VLE calculation mole fraction in the gas phase

yexp - calculated from experimental analysis mole fraction in the gas phase

z_i - total mole fraction of *i* species at the reactor exit

Z - compressibility factor (eqn. A.14)

<u>*Greek*</u>

$\alpha_i(T)$ - scaling factor defined by eqn. A.8

Δ - means components, which were measured experimentally in the liquid phase

ε - criterion for convergence

$\hat{\phi}_i$ - fugacity coefficient of species *i*

υ - molar volume, $m^3\ mol^{-1}$

Ω - set of species that were included in VLE calculation (H_2, CO, CO_2, water, paraffins $C_{1\text{-}20}$, 1-olefins $C_{2\text{-}15}$, lumped pseudo-component C_{21}^{+}, pseudo-component unanalyzed wax and Durasyn)

ω - acentric factor for pure component

Superscripts

avg - average

aqu - in a aqueous phase

calc - calculated

exp - experimental

G - in a gas phase

L - in a liquid phase

min - minimum

max - maximum

norm - normalized by equation (5)

org - in a organic phase

tail - in a tail gas phase, gas phase under the normal (standard) conditions (273.15°K, 101325 Pa)

v - vapor

wax - in a wax phase

Subscripts

c - critical property

i,j,k - component identifications

r - reduced property

VLE - vapor-liquid equilibrium calculation

Appendix A

Modified Peng-Robinson Equation of State

Peng and Robinson (1976) proposed the EOS of following form:

$$p = \frac{RT}{\upsilon - b} - \frac{a}{\upsilon(\upsilon + b) + b(\upsilon - b)} \tag{A.1}$$

where: p = pressure; T = temperature, υ = molar volume. Parameters *a* and *b* are correlated with critical properties of components and follow the mixing rules. The mixing rules are

$$a = \sum_{i=1}^{v} \sum_{j=1}^{v} z_i \cdot z_j \cdot a_{i,j} \tag{A.2}$$

$$a_{i,j} = \left(a_i \cdot a_j\right)^{0.5} \cdot \left(1 - k_{i,j}\right) \tag{A.3}$$

$$a_i = a_{c,i} \cdot \alpha_i(T) \tag{A.4}$$

$$a_{c,i} = \frac{0.45724 \cdot R^2 {T_{c,i}}^2}{P_{c,i}} \tag{A.5}$$

$$b = \sum z_i \cdot b_i \tag{A.6}$$

$$b_i = \frac{0.0778 \cdot R \cdot T_{c,i}}{P_{c,i}} \tag{A.7}$$

where z is a mole fraction of species in the liquid x or in the gas y, T_c and P_c are the critical temperature and pressure for pure component, $k_{i,j}$ is a binary interaction factor between two species and temperature dependent coefficient α is:

$$\alpha_i(T) = \left(1 + f_i(\varpi) \cdot \left(1 - T_{r,i}^{0.5}\right)\right)^2 \tag{A.8}$$

where $T_{r,i}$ is reduced temperature, $T_{r,i} = T/T_{c,i}$ (T and T_c are in *K*) and $f_i(\varpi)$ is a function of acentric factor ω,

$$f_i(\varpi) = 0.37464 + 1.54226 \cdot \omega_i - 0.26992 \cdot {\omega_i}^2 \tag{A.9}$$

Li and Froment (1996) proposed the following modification of $f_i(\varpi)$ function (for permanent gases and water only):

$$f_i(\varpi) = 0.3608281 + 1.14748 \cdot \omega_i - 0.5005316 \cdot {\omega_i}^2 - 0.04187888 \cdot {\omega_i}^3 \quad \text{(A.10)}$$

The equation A.1 can be expressed in dimensionless form by introducing a compressibility Z as follows:

$$Z^3 - (1 - B) \cdot Z^2 + \left(A - 2A - 3B^2\right) \cdot Z - \left(AB - B^2 - B^3\right) = 0 \quad \text{(A.11)}$$

where the dimensionless parameters *A* and *B* are

$$A = \frac{a \cdot P}{R^2 T^2} \quad \text{(A.12)}$$

$$B = \frac{b \cdot P}{R \cdot T} \quad \text{(A.13)}$$

and the compressibility factor is:

$$Z = \frac{P \cdot \upsilon}{R \cdot T} \quad \text{(A.14)}$$

Equation A.11 yields one root for a one-phase system or three roots for a two-phase mixture system. In case of the two-phase region, the largest root gives the compressibility factor *Z* of the vapor, whereas the smallest positive one gives the compressibility factor *Z* of the liquid.

Appendix B

Critical properties of Durasyn 164 oil

Durasyn 164 oil was used as a start-up fluid in the STSR tests of the Ruhrchemie catalyst, and it is present in the liquid withdrawn from the reactor during Fischer-Tropsch synthesis. Its critical properties and acentric factor are needed for the VLE calculations. The following information was obtained from the Amoco (BP group) Co. (manufacturer of Durasyn):

- Durasyn is a mixture of polyalfaolefins; i.e. mixture of 1-decene dimers, trimers, tetramers and higher oligomers.
- Its boiling point is 375 °C to 505 °C
- Average molecular weight is ~ 420 g/mol

In order to estimate the properties needed for the VLE calculations it was assumed that Durasyn is 1-decene trimer (416.8 g/mol). The structure of 1-decene trimer is shown in Figure B.1.

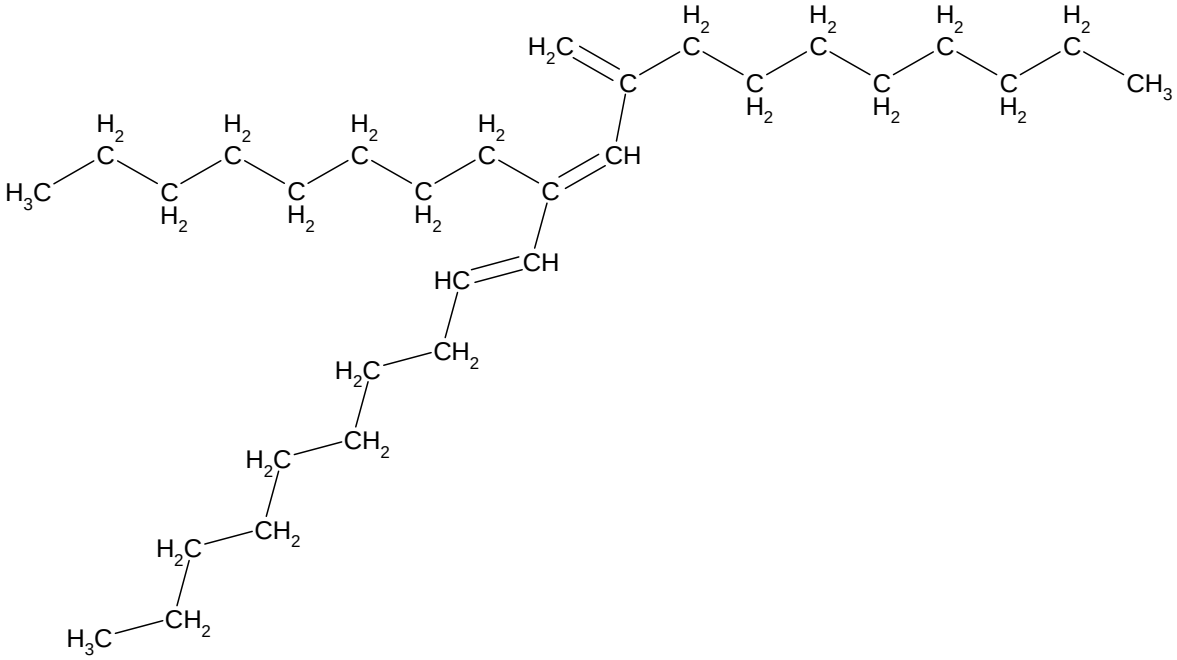

Figure B.1. 1-Decene trimer structure

Critical pressure

We have used Joback's group contribution method to calculate the critical pressure of Durasyn (Joback, 1984; Joback and Reid 1987). The Joback's method is modification of the Lydersen's method (Poling *et al*., 2001). According to this method the critical pressure is calculated as:

$$P_c(bar) = \left[0.113 + 0.0032 \cdot N_{atoms} - \sum_k N_k \cdot (pck) \right]^{-2} \quad \text{(B.1)}$$

where N_k and pck are group number and group contribution, respectively; N_{atoms} is a total number of atoms in molecule. The *pck*-values are provided contributors and they are characteristic for particular molecule group. Parameter values as well as groups and atom numbers needed for calculation of critical properties of Durasyn are provided in Table B.1.

Table B.1. Parameters needed for Joback's Method (Poling et al., 2001).

Groups	N_k	*tck*	*pck*	N_{atoms}
-CH3	3	0.0141	-0.0012	12
=CH2	1	0.0113	-0.0028	3
=CH-	3	0.0129	-0.0006	6
=C<	2	0.0117	0.0011	2
-CH2-	21	0.0189	0	63
Total	30			86

Average error for compounds with 3 or more carbon atoms is less then 5% (Poling *et al*., 2001). The critical pressure predicted by this method for n-paraffins is in very good agreement with experimental data reported in the literature (Reid *et al*., 1977; Ambrose and Tsonopoulos, 1995; Passut and Danner, 1973; Poling *et al*., 2001; Nikitin *et al*., 1997; Gao *et al*., 1999, 2001) as shown in Figure B.2. Comparison of Joback's method with other methods for n-paraffin critical pressure is also shown in this figure. Experimental data in Figure B.2 are indicated by triangular points. Lydersen (1955), Marano and Holder (1997), Gao *et al*. (2001) and Joback's (Joback, 1984; Joback and Reid 1987) methods (lines in Fig. B.2) are predictions. Lydersen and Joback's methods are group contribution methods and can be used for a wide range of species (like

branched hydrocarbons), whereas Marano and Holder and Gao *et al.* predictions are valid only for n-paraffins (they are the asymptotic behavior correlation (ABC) methods).

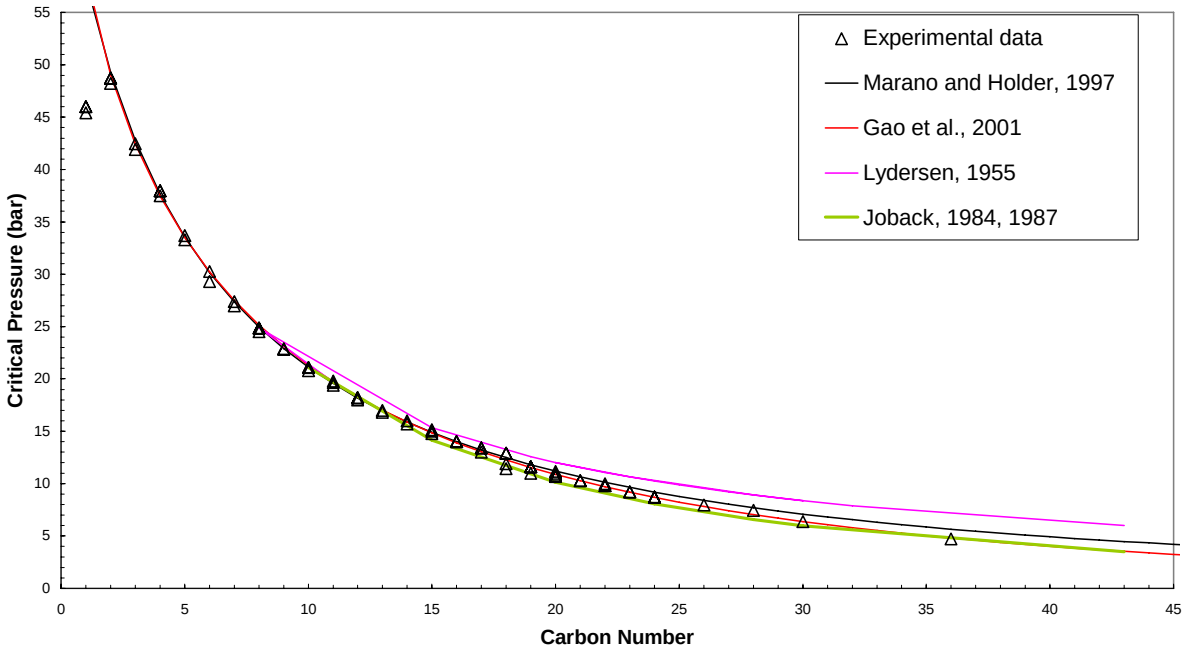

Figure 2. Predictions of the critical pressure of n-paraffins.

Critical temperature

We have used two group contribution methods to calculate the critical temperature: Joback (Joback, 1984; Joback and Reid, 1987) and Klincewicz's method (Klincewicz and Reid, 1984).

Joback's method requires a boiling point and structure of a molecule to predict the critical temperature of a compound:

$$T_c(K) = T_b(K) \cdot \left[0.584 + 0.965 \cdot \left\{ \sum_k N_k \cdot (tck) \right\} - \left\{ \sum_k N_k \cdot (tck) \right\}^2 \right]^{-1} \qquad \text{(B.2)}$$

where N_k and tck are group number and group contribution, respectively; T_b is a boiling point. Average error for compounds with 3 or more carbon atoms is 1.1% (Poling *et al.*, 2001). The critical temperature predicted by this method for n-paraffins is in good agreement with experimental data up to C_{24}, but beyond C_{28} the error is greater then 5%. Therefore, we also used

the Klincewicz's method to calculate the critical temperature of Durasyn, since it is more accurate for n-paraffins around C_{30}, but is less accurate for paraffins up to C_{24} (Figure B.3). Besides the boiling point and the structure of molecule, this method requires a molecular weight of the compound:

$$T_c(K) = 45.40 - 0.77 \cdot MW(g/mol) + 1.55 \cdot T_b(K) + \left\{ \sum_k N_k \cdot (tck) \right\} \quad \text{(B.3)}$$

where N_k and *tck* are group number and group contribution, respectively; T_b is a boiling point; MW is a molecular weight of compound. The N_k and *tck*-values for Durasyn are shown in Table B.1.

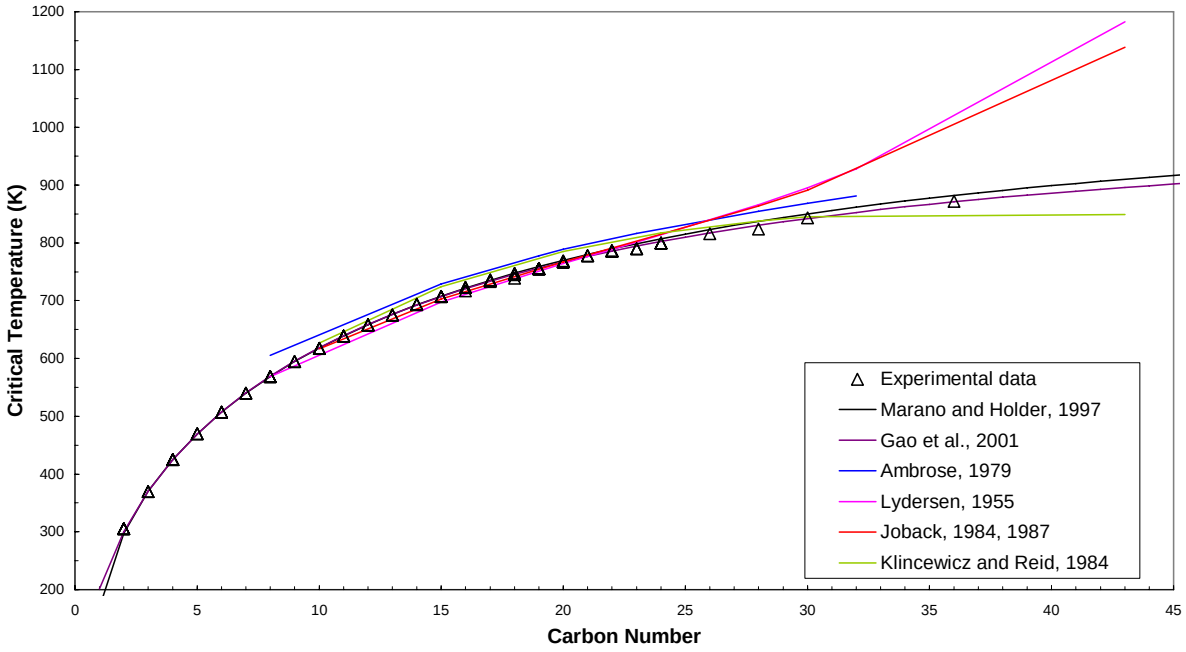

Figure B.3. Predictions of the critical temperature for n-paraffins.

A comparison of these two (Joback's and Klincewicz's) and other prediction methods with experimental data is shown in the Figure B.3 for n-paraffins. Experimental data are designated with triangular points, whereas solid lines are predictions. Ambrose (1979), Lydersen (1995), Joback (Joback, 1984; Joback and Reid 1987) and Klincewicz's (Klincewicz and Reid, 1984) are group contribution methods and can be used for prediction of properties of different types of

hydrocarbons. Marano and Holder (1997) and Gao *et al*. (2001) are ABC (asymptotic behavior correlation) methods that can be used only for n-paraffins. As can be seen the ABC methods provide more accurate predictions for n-paraffins but can't be used for predictions of critical properties of branched hydrocarbons.

Both of these methods (Joback's and Klincewicz's) give almost the same result for the maximum value of the critical point and similar values for the minimum T_c. However, the critical temperature range calculated by the Joback's method is more narrow than the one calculated from the Klincewicz's method (Table B.2). We used the average critical temperature calculated from the Joback's method for the VLE calculations.

Table B.2. Predicted critical properties for Durasyn.

	P_c, bar	T_c, K		T_c^{avg}
Joback	6.44	794.4	953.7	874.1
Klincewicz	-	751.5	953.0	852.2

where T_c^{avg} is the average critical temperature $T_c^{avg} = \left(T_c^{\min} + T_c^{\max}\right)/2$.

Acentric Factor (ω)

Several methods are available for prediction of an acentric factor. Comparison of predicted values with experimental data for n-paraffins is shown in Figure B.4. Experimental data are represented by triangular points, and predictions by solid lines. Gao *et al*. (2001) and Marano and Holder (1997) methods can predict acentric factor for n-paraffins only. Gao *et al*.'s model has the best accuracy for n-paraffins experimental data. Edmister (1958), Ambrose and Walton (1989) and Lee and Kesler (1975) methods require the critical pressure, critical temperature and boiling point temperature for prediction of the acentric factor, but they can be used to predict acentric factors for different types of organic species. Ambrose and Walton's and Lee and Kesler's method have similar accuracy and are more accurate than Edmister's method for n-paraffins up to C_{20} (Fig. B.4). These two methods were used for calculation of the acentric factor of Durasyn.

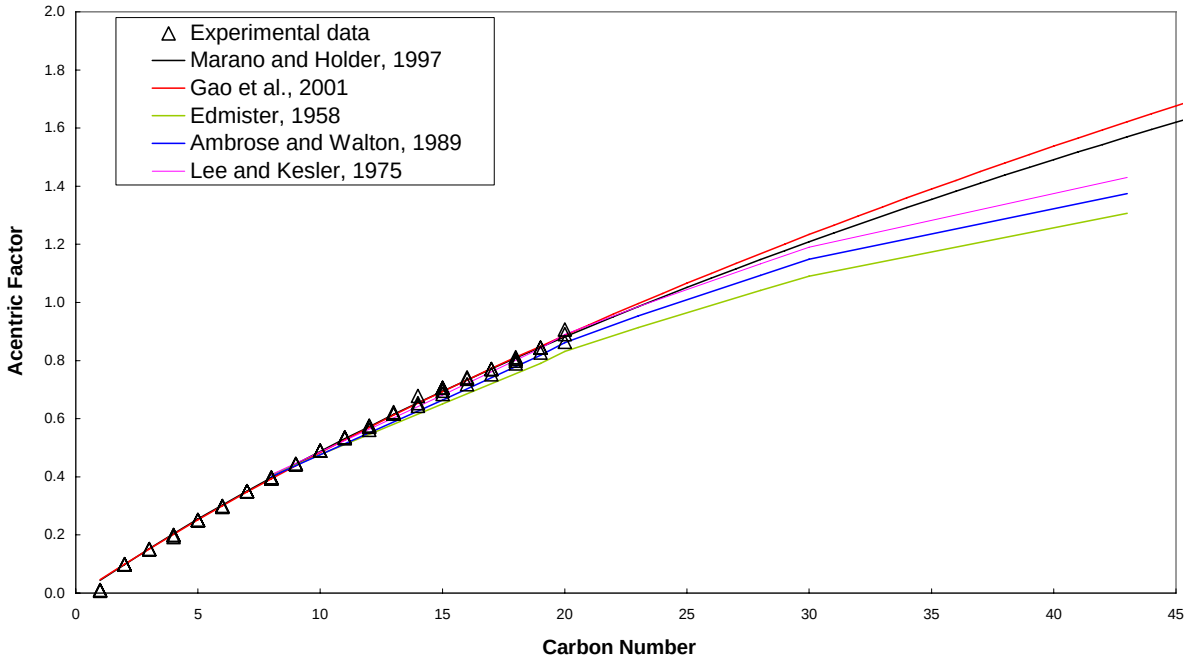

Figure B.4. Predictions of the acentric factor for n-paraffins.

The critical pressure and the critical pressure, and ratio of the boiling point to the critical temperature (T_b/T_c) of Durasyn were calculated by Joback's method. The ratio of T_b/T_c is equal to 0.816. Calculated acentric factors are shown in Table B.3.

Table B.3. Predicted values of the acentric factor for Durasyn.

Acentric factor (ω)	
Ambrose and Walton	0.546
Lee and Kesler	0.569

For the VLE calculations we used the critical pressure and the average critical temperature from the Joback's method, and the acentric factor from the Lee and Kesler's method (Table B.4).

Table B.4. Properties of Durasyn for the VLE calculations.

P_c, bar	T_c, K	ω
6.44	874.1	0.569

The corresponding experimental values of critical properties for C_{30} n-paraffin are: T_c = 843 K, P_c = 6.36 bar, whereas the calculated value of the acentric factor is ω =1.233.

Appendix C

Calculation of the vapor-liquid equilibrium

Definitions and Notation

There are two phases in the reactor under the reaction conditions: the gas phase and the liquid phase (Figure C.1). The gas phase in the reactor consists of components that are measured at the exit of the reactor in one of the three phases: tail gas, aqueous phase and organic phase (see Figure 2). The gas phase components are: inorganic species (H_2, CO, CO_2, H_2O) and hydrocarbons (up to ~ C_{30}). The liquid phase in the reactor consists of wax (high molecular weight products produced during F-T synthesis) and the start-up fluid (Durasyn).

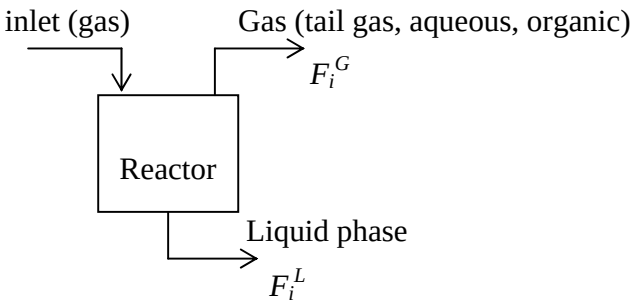

Figure C.1. Reactor schematics for the VLE calculations

Molar flow rate of *i* component in the gas phase F_i^G (*mol/h*), is calculated as follows

$$F_i^G = F_i^{tail} + F_i^{aqu} + \cdot F_i^{org} \tag{C.1}$$

whereas for the liquid phase F_i^L (*mol/h*) is

$$F_i^L = F_i^{wax} \tag{C.2}$$

where "wax" refers to analyzed hydrocarbons ($C_{10\text{-}50}$), unanalyzed wax and Durasyn.

The following species were taken into account in the VLE calculations: inorganic species (H_2, CO, CO_2, H_2O), n-paraffins (C_1-C_{20}), 1-olefins (C_2-C_{15}), Durasyn (C_{30}) and two pseudo-components: C_{21}^+ paraffins and unanalyzed wax (with critical properties and acentric factor of

C_{30} n-paraffin). Thus, the VLE calculations were done for a two-phase mixture of 41 components (species).

The pseudo-component C_{21}^{+} represents lumped hydrocarbons (up to C_{50}) and its molar flow rate is calculated as a sum of molar flow rates of paraffins from C_{21} to C_{50} (some of these are present in both the gas and the liquid phase):

$$F_{C_{21}+}^{G,L} = \sum_{i=21}^{50} F_i^{G,L} \tag{C.3}$$

where superscripts *G* and *L* denote vapor and liquid phases, respectively.

The unanalyzed wax was treated like n-paraffin with 30 carbon atoms, whereas critical properties of Durasyn were calculated as described in Appendix B.

Experimental values of mole fractions in the gas and liquid phases were calculated as follows:

$$y_i^{\exp} = \frac{F_i^G}{\sum_{i\in\Omega} F_i^G} \tag{C.4}$$

$$x_i^{\exp} = \frac{F_i^L}{\sum_{i\in\Omega} F_i^L} \tag{C.5}$$

were F^G and F^L represent molar flow rates of species in the gas and liquid phase, respectively; Ω represents the set of species that were included in VLE calculation (H_2, CO, CO_2, water, paraffins $C_{1\text{-}20}$, 1-olefins $C_{2\text{-}15}$, lumped pseudo-component C_{21}^{+}, pseudo-component unanalyzed wax and Durasyn).

However, experimental molar flow rates are not available for all components in both phases present in the reactor. For example inorganic species and lower molecular weight hydrocarbons (~C_1-C_9) were not analyzed in the liquid phase, whereas high molecular weight hydrocarbons (>C_{30}) are not detected in the products leaving the reactor as the gas phase (Figure C.1). Therefore, we need to apply some method to calculate molar flow rates of all species in the liquid and the gas phase. This is accomplished through VLE calculations.

VLE Calculations Procedure

Figure C.2 illustrates the input and output variables in VLE calculations.

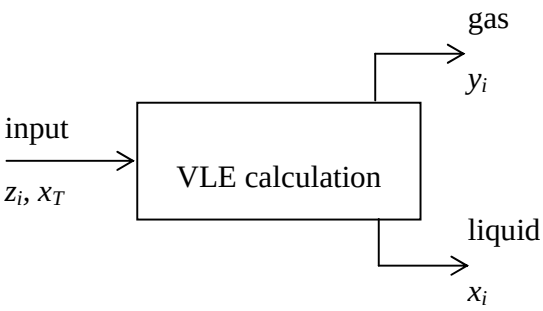

Figure C.2. VLE calculations schematic

Total mole fraction of component *i* (z_i) at the reactor exit is calculated as follows:

$$z_i = \frac{F_i^G + F_i^L}{\sum_i \left(F_i^G + F_i^L\right)} \tag{C.6}$$

Mole fraction of the liquid phase (x_T) is given by:

$$x_T = \frac{\sum_i F_i^L}{\sum_i \left(F_i^G + F_i^L\right)} = \frac{F_T^L}{F_T} \tag{C.7}$$

whereas the total mole fraction of the gas phase is:

$$y_T = 1 - x_T \tag{C.8}$$

Assuming that the gas and the liquid phase are in thermodynamic equilibrium one has to solve the following set of equations:

$$\frac{y_i}{x_i} = \frac{\hat{\phi}_i^L(x_i)}{\hat{\phi}_i^G(y_i)} \tag{C.9}$$

$$x_i \cdot x_T + y_i \cdot (1 - x_T) = z_i \tag{C.10}$$

This is the nonlinear set of equations where fugacity coefficients $\hat{\phi}_i^L(x_i), \hat{\phi}_i^G(y_i)$ are functions of P, T and composition. The total mole fraction of species z_i and total mole fraction of liquid phase x_T are known from the product analysis, whereas mole fractions of species in the liquid (x_i) and gas (y_i) are unknown.

Algorithm for calculation of vapor-liquid equilibrium

1. Guess initial values of the mole fractions of all species in the liquid and the gas phase

$$x_i, y_i$$

2. Solve the modified Peng –Robinson EOS and calculate fugacity coefficients in the gas $\hat{\phi}_i^V$ and liquid phase $\hat{\phi}_i^L$ corresponding to the current values of x_i and y_i.

Inputs into this subroutine are: composition of the liquid and gas phase; the system temperature and pressure, as well as critical properties (temperature, pressure, acentric factor) of all species.

3. Calculation of *K*-values:

$$K_i = \frac{\hat{\phi}_i^L}{\hat{\phi}_i^V}. \tag{C.11}$$

4. Calculation of "new" x_i and y_i values:

$$x_i = \frac{z_i}{x_T + K_i \cdot (1 - x_T)} \tag{C.12}$$

$$y_i = K_i \cdot x_i \tag{C.13}$$

Equation (C.12) is obtained from mass balance on species *i* at the exit as follows:

Molar flow rate of *i* in the liquid + Molar flow rate of *i* in the gas = Molar flow rate of *i* in the overall flux at the reactor exit, i.e.:

$$x_i \cdot F_T^L + y_i \cdot F_T^G = z_i \cdot \left(F_T^L + F_T^G\right) \tag{C.14}$$

where: F_T^L, F_T^G are the total molar flow rates of the liquid and the gas phase, respectively.

Divide (C.14) by the total molar flow rate at the reactor exit ($F_T = F_T^L + F_T^G$), to obtain:

$$x_i \cdot x_T + y_i \cdot y_T = z_i \tag{C.15}$$

Combining (C.6) and (C.13) we obtain:

$$x_i \cdot x_T + x_i \cdot K_i \cdot (1 - x_T) = z_i$$

which after rearrangement leads to (C.12).

Equation (C.11) follows from the definitions of the K-value and fugacity coefficients:

$$K_i \equiv \frac{y_i}{x_i} \tag{C.16}$$

$$y_i \cdot \hat{\phi}_i^V \cdot P = x_i \cdot \hat{\phi}_i^L \cdot P \tag{C.17}$$

In equilibrium: $\hat{f}_i^V = \hat{f}_i^L$, and combining the last two equations one obtains (C.11).

5. Checking of objective function for convergence. If the objective function is less or equal to criterion for convergence ε then finish.

$$if \left(S_{VLE} = \sum_i \left| \hat{f}_i^V - \hat{f}_i^L \right| \le \varepsilon \right) then\ finish \tag{C.18}$$

where $\hat{f}_i^V$ and $\hat{f}_i^L$ are fugacities of *i* species in the vapor and liquid phase, respectively.

6. If (C.18) is not satisfied go back to step 2 and keep on iterating until the criterion for convergence is satisfied.

As an illustration of the above procedure we show results from one set of calculations (Table C.1 and Figure C.3). Additional results (in graphical form) are shown in the Results and Discussion section of the report (Figures 11 and 12).

Table C.1. Example of VLE calculation

MB: 21903_001

xT: 0.0109369 - mole fraction of total liquid at the exit (Input to subroutine)

		Input	Experimental values		Output - calculated values			
Group	**Carbon #**	**z**	**yexp**	**xexp**	**y**	**x**	**K**	**xnorm**
Carbon Monoxide		0.4268405	0.43156	0	0.43068	0.024686	17.45	
Hydrogen		0.2495477	0.252307	0	0.251793	0.011932	21.10	
Carbon Dioxide		0.2200364	0.222469	0	0.222016	0.024698	8.99	
Water		0.051163	0.051729	0	0.051623	0.011289	4.57	
paraffin	1	0.0114569	0.011584	0	0.01156	0.00099	11.68	
	2	0.0033668	0.003404	0	0.003397	0.000471	7.22	
	3	0.0011265	0.001139	0	0.001137	0.000231	4.93	
	4	0.0006931	0.000701	0	0.000699	0.000207	3.37	
	5	0.0004922	0.000498	0	0.000497	0.000212	2.34	
	6	0.0003209	0.000324	0	0.000324	0.000197	1.64	
	7	0.000271	0.000274	0	0.000273	0.000236	1.16	
	8	0.0003744	0.000379	0	0.000378	0.000461	0.819	
	9	0.0004623	0.000467	0	0.000466	0.000801	0.582	
	10	0.0003244	0.000315	0.001151	0.000319	0.000772	0.414	0.000842
	11	0.0002698	0.000255	0.001579	0.000263	0.000882	0.298	0.000963
	12	0.0002293	0.00021	0.002009	0.00022	0.001045	0.211	0.00114
	13	0.0002199	0.000194	0.002605	0.000207	0.001382	0.150	0.001508
	14	0.0002136	0.00018	0.00326	0.000196	0.001841	0.106	0.002009
	15	0.0001954	0.000155	0.003852	0.000173	0.002249	0.0768	0.002454
	16	0.0001826	0.000131	0.004863	0.000154	0.002779	0.0554	0.003033
	17	0.0001652	0.000105	0.005644	0.000132	0.003201	0.0411	0.003494
	18	0.0001533	8.32E-05	0.006494	0.000114	0.003698	0.0309	0.004036
	19	0.0001325	6.25E-05	0.006457	8.85E-05	0.00411	0.0215	0.004487
	20	0.0001122	4.6E-05	0.006094	6.41E-05	0.004461	0.0144	0.004869
1-olefin	2	0.003509	0.003548	0	0.003541	0.000434	8.15	
	3	0.006693	0.006767	0	0.006753	0.001291	5.23	
	4	0.0036065	0.003646	0	0.003639	0.001009	3.61	
	5	0.0021617	0.002186	0	0.002181	0.00087	2.51	
	6	0.0014214	0.001437	0	0.001434	0.000827	1.73	
	7	0.0009928	0.001004	0	0.001002	0.000798	1.26	
	8	0.0007179	0.000726	0	0.000724	0.00081	0.894	
	9	0.0008199	0.000829	0	0.000827	0.001372	0.603	
	10	0.0004638	0.00046	0.000768	0.000457	0.001036	0.441	0.001131
	11	0.0002408	0.000234	0.000863	0.000235	0.000767	0.306	0.000837
	12	0.000197	0.000189	0.000881	0.00019	0.000825	0.230	0.000901
	13	0.0001451	0.000138	0.000829	0.000137	0.000887	0.154	0.000968
	14	0.0001064	9.91E-05	0.000768	9.76E-05	0.000896	0.109	0.000978
	15	7.362E-05	6.95E-05	0.000448	6.52E-05	0.000834	0.0782	0.00091
lumped C21+		0.0007026	9.65E-05	0.055512	5.47E-05	0.059292	0.0009	0.064717
unanalyzed wax		0.0013133	0	0.12008	7.49E-05	0.110604	0.0007	0.120723
Durasyn		0.0084854	0	0.775844	0.001813	0.714619	0.0025	0.78

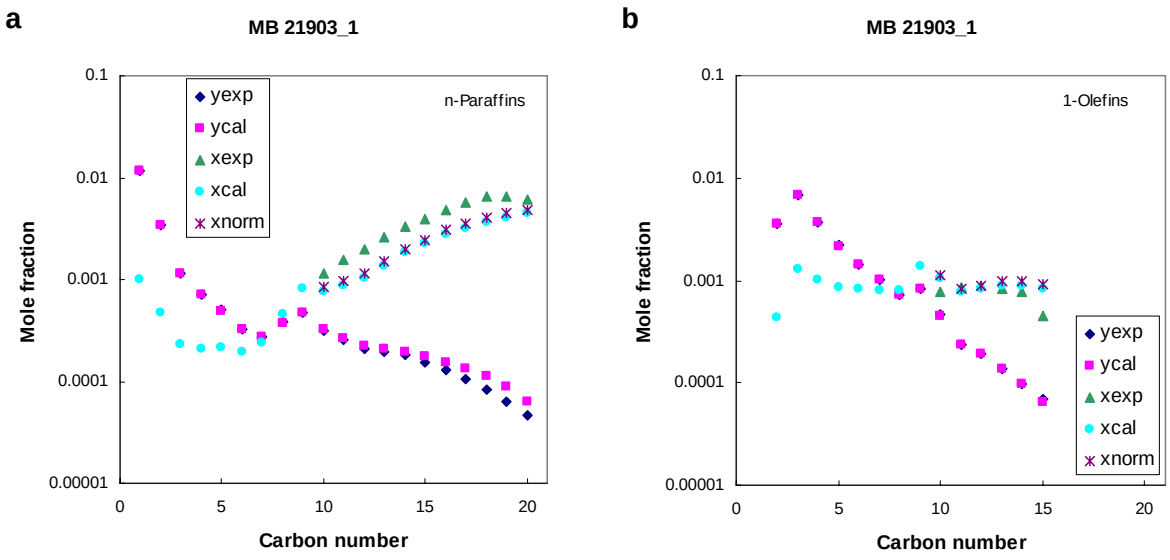

Figure C.3. Example of VLE calculation result for MB 21903_1. Reaction conditions: 260°C, 1.48 bar, 0.667 H_2/CO and SV = 4 Nl/g_{Fe}/h

Table C.1 shows all input values for the VLE calculations (xT and the overall mole fractions for all 41 components considered in the VLE calculations) and the results of the VLE calculations (mole fractions in the liquid phase and the vapor phase, and the corresponding K values). In columns 5 and 6 of this Table are experimental values in the gas phase and the liquid phase, respectively. The last column contains the normalized values of calculated mole fractions in the liquid phase defined by equation (5) in the Results and Discussion section of the report. It can be noted that the calculated values for the inorganic species in the gas phase are in excellent agreement with the corresponding experimental values.

Comparison of calculated and experimental values for hydrocarbons (except for C_{21}^+, unanalyzed wax and Durasyn) is shown in Figure C.3. There is very good agreement between the calculated and experimental values for the gas phase over a wide range of carbon numbers, whereas larger differences are observed for the liquid phase composition. We believe that the latter is caused by experimental errors in quantification of the liquid phase components (including Durasyn and wax).